

Minimal superfluid vortices in chiral perturbation theory

Fabrizio Canfora,^{1,2,*} Martín Garrido,^{3,†} Massimo Mannarelli,^{4,‡} and Anibal Neira^{3,§}

¹*Centro de Estudios Científicos (CECS), Casilla 1469, Valdivia, Chile*

²*Universidad San Sebastián, sede Valdivia, General Lagos 1163, Valdivia 5110693, Chile*

³*Universidad de Concepción (UDEC), Concepción, Chile*

⁴*Laboratori Nazionali del Gran Sasso, INFN, Via G. Acitelli 22, Assergi (AQ), I-67100, Italy*

We derive some properties of rotational vortices in the pion condensed phase. Employing leading order chiral perturbation theory we determine the minimal energy condition for vortex nucleation. Vortices have quantized angular momentum along the rotation axis, an hallmark of superfluidity, and self-confine pions. The critical rotation frequency for vortex nucleation is estimated.

I. INTRODUCTION

The theoretical understanding of the phases of strongly interacting matter at different temperature, baryonic density and isospin asymmetry is one of the major challenges in particle physics. Many of the most important open problems in quantum-chromodynamics (QCD) are indeed deeply linked to the possible realization of the different phases of hadronic matter. For instance, the mechanism underlying color confinement can be explored studying the high-temperature transition between standard hadronic matter and the quark-gluon plasma (QGP) [1–8], or determining whether a low-temperature high-density transition to quarkyonic [9] or color superconducting [10–13] matter occurs. Unfortunately, these phase transitions cannot be attacked by perturbative methods: at the relevant energy scales QCD is nonperturbative. Therefore, alternative methods must be used.

Numerical lattice QCD (LQCD) simulations allow to explore a sizable part of the hadronic matter phase diagram [14, 15]. However, the so-called sign problem limits the region of parameter space where this method can be used [3, 4, 16–20]. In particular, investigating hadronic matter as a function of the baryonic chemical potential is challenging [21]. This means that the quarkyonic phase as well as the color superconducting phase remain, so far, inaccessible. On the other hand, there is no numerical problem in Monte Carlo simulations at vanishing baryonic density and nonzero isospin chemical potential, μ_I [22]. Such system can be viewed as made of strongly interacting pions, which are stable because the weak interaction has been turned off. At sufficiently low temperature it happens that for isospin chemical potential exceeding the pion mass, m_π , pions form an homogeneous Bose-Einstein condensate (BEC). This phase was already proposed in the 1970s [23–27] as the ground state of extremely high-dense nuclear matter. Although its possible realization is still controversial, see for instance [28], nevertheless it represents a formidable portal

to inquiry the properties of hadronic matter. One of the reasons is that it can be studied by means of several and somehow complementary methods: Chiral perturbation theory (χ PT) [29–46], NJL models [47–70], linear σ and quark-meson models [71–77], random matrix models [78, 79], ladder QCD [80] and holographic QCD [81–83] allow to understand many features of meson condensation. The findings of effective theories align with LQCD results [84–101] for $\mu_I \gtrsim m_\pi$, and this fact makes our description of the pion condensed phase robust. In particular, it is well established that there exists a second order phase transition between the naive vacuum and the pion condensed phase [32, 33]. In the range $\mu_I \gg m_\pi$, the errors in LQCD simulations become large, however they show qualitative agreement with the outcomes of perturbative methods [102–104].

One of the benefits of effective theories is that they allow to handle the properties of topological objects. These are of great importance because they encode valuable information on the non-perturbative sector of a theory [6–8, 105–108]. A prototypical example is the case of vortices in type II superconductors [105, 108]. Superconducting vortices with quantized magnetic flux present in the mixed phase characterize the response of these systems to an external magnetic field. However, the theoretical description of type II superconductors is challenging as the actual mechanism underlying superconductivity is poorly understood. The simplest theory, the one elaborated by Bardeen, Cooper and Schrieffer (BCS), can qualitatively describe various properties of type I superconductors, but struggles with type II superconductors, which are typically realized with complex materials.

A powerful technique to study such topological configurations was provided by Bogomol'nyi, Prasad and Sommerfield (BPS), that obtained the minimum energy of soliton configurations, known as the BPS bound. In this case, the actual expression of interactions becomes immaterial, insofar they allow the realization of the broken phase. This happens at a particular value of the system parameters, called the BPS critical point. In case of superconducting vortices it corresponds to the critical point between Type II and Type I superconductors. In the Ginzburg–Landau theory, the penetration lengths of the scalar and vector gauge fields are equal, the ground state is then determined by the solution of first order non-

* fabrizio.canfora@uss.cl

† margarrido2021@udec.cl

‡ massimo.mannarelli@lngs.infn.it

§ aneira2017@udec.cl

linear differential equations, instead of the typical second order field equations. A further advantage to deal with solitons at the BPS critical point is that this condition allows to study the low-energy dynamics using the so-called moduli-space approximation, see [109–111]. Moreover, the analysis of interaction of solitons with fermions is simplified by powerful index theorems [105, 108]. Thus, the theory of BPS solitons is not just a mathematical curiosity but rather a very efficient tool for the analysis of nonperturbative states. It can be applied to standard superfluids described by the Gross-Pitaevskii (GP) equation [112–116]. A BPS bound was indeed derived in two-dimensional GP theory [117, 118] together with the corresponding first order BPS differential equations. These results suggest that a similar construction could work in χ PT [119, 120]. Using χ PT minimally coupled to electromagnetism has been possible to find the BPS bound in two different systems of pions [121, 122].

In the present paper we employ leading order χ PT at the critical BPS point to show that the pion condensed phase can host quantized vortices. Considering cylindrical Minkowskian space-time at vanishing temperature, vortex solutions with minimal free-energy cost are found by appropriately tuning the isospin chemical potential. Remarkably, the results we obtain show close analogy with those long studied in standard superfluids and in dilute ultracold atoms: the total angular momentum is quantized and vortex nucleation happens at a critical frequency. The main – and quite interesting – different feature is that matter confinement is not determined by an external vessel or a trap, it is instead self-induced by the pion interaction.

This paper is organized as follows. In Sec. II we introduce the χ PT theoretical setup and we briefly recap the main features of the well-known homogeneous pion condensed phase. In Sec. III we derive the BPS bound in χ PT at nonvanishing isospin chemical potential. In Sec. IV we construct superfluid single vortex solutions at the BPS critical point. More general vortex structures are discussed in Sec. V, while the free energy and the critical rotation frequency are studied in Sec. VI. We draw our conclusions in Sec. VII. In the Appendix we provide some details of the calculation of the angular momentum of noncentral vortices. We employ natural units $c = \hbar = 1$.

II. THEORETICAL SET-UP

A system of pions at vanishing temperature in Minkowski spacetime \mathcal{M} can be described by the χ PT action

$$S = \int_{\mathcal{M}} d^4x (K \text{Tr} [L^\mu L_\mu^\dagger] + V), \quad (1)$$

which only includes the leading $O(p^2)$ terms and it is valid for momenta $p \ll \Lambda_\chi$, where $\Lambda_\chi \sim 1$ GeV is the χ PT breaking scale, see [123–131]. Here, $K = f_\pi^2/4$, with f_π the pion decay constant and V the potential that

will be specified below. The derivative term has been conveniently written by means of

$$L_\mu = U^{-1} D_\mu U, \quad (2)$$

where $U(x) \in SU(2)$ is an isospin representation of the pion fields, while the covariant derivative

$$D_\mu U = \partial_\mu U + i \frac{\mu_I}{2} [\sigma_3, U] \delta_{\mu 0}, \quad (3)$$

includes the contribution of the isospin chemical potential. This can be viewed as a time-like external vector field proportional to the Pauli matrix σ_3 . It explicitly breaks boost invariance, because it is proportional to $\delta_{\mu 0}$, and the $SU(2)$ isospin symmetry: the Lagrangian is solely invariant under transformations of the $U(1)$ subgroup generated by σ_3 ; see [28] for more details.

By comparison with LQCD results, one finds that Eq. (1) allows to accurately describe the low-energy properties of pions for $\mu_I \lesssim 1.2m_\pi$; higher values of the isospin chemical potential require additional terms in the action, see for instance [132]. In the representation

$$U = \mathbf{1} \cos \alpha + i \mathbf{n} \cdot \boldsymbol{\sigma} \sin \alpha, \quad (4)$$

where $\mathbf{1}$ denotes the 2×2 identity matrix, $\boldsymbol{\sigma}_i$ for $i = 1, 2, 3$ are the Pauli matrices and pions are grouped in the unit vector

$$\mathbf{n} = \{\sin \Theta \cos \Phi, \sin \Theta \sin \Phi, \cos \Theta\}, \quad (5)$$

where $\alpha = \alpha(x^\mu)$, $\Theta = \Theta(x^\mu)$, $\Phi = \Phi(x^\mu)$ are three real scalar fields. In order to make contact with the standard representation of pions, it is useful to compare Eqs. (4) and (5) with

$$U = \exp \left(i \frac{\boldsymbol{\sigma} \cdot \boldsymbol{\varphi}}{f_\pi} \right), \quad (6)$$

where $\boldsymbol{\varphi} = (\varphi_1, \varphi_2, \varphi_3)$ are three scalar fields and pions correspond to

$$\pi_0 = \varphi_3 \quad \pi_\pm = \frac{\varphi_1 \pm i\varphi_2}{\sqrt{2}}. \quad (7)$$

Matching the two representations we have that $\pi_0 = \varphi_3 = f_\pi \cos \Theta$ and thus the neutral pion depends solely on the Θ field. A system without the condensation of neutral pions corresponds to $\Theta = \pi/2$. Since neutral pions are states with $I_3 = 0$, at tree level they are insensitive to the isospin chemical potential. In the following we will be interested to the phases that appear as a response to a nonvanishing isospin chemical potential, thus taking $\varphi_3 = 0$ is a reasonable assumption; as will be shown hereafter, it corresponds to a minimum of the free energy. For vanishing neutral pion component, we have that

$$\alpha e^{\pm i\Phi} = \sqrt{2} \frac{\pi_\pm}{f_\pi}, \quad (8)$$

and therefore

$$\alpha = \frac{\sqrt{2}}{f_\pi} \pi_+ \pi_- \quad \text{and} \quad \tan \Phi = i \frac{\pi_+ + \pi_-}{\pi_- - \pi_+}, \quad (9)$$

meaning that α describes the absolute value of the pion condensate, while Φ its phase.

Although Eq. (6) is useful to describe pion interactions, the ground state properties are more easily studied using Eq. (4). With such parametrization, the Lagrangian density in Eq. (1) can be written as

$$\mathcal{L} = \mathcal{L}_k + \mathcal{L}_V, \quad (10)$$

with the derivative term given by

$$\begin{aligned} \mathcal{L}_k = & 2K \left[\partial_\mu \alpha \partial^\mu \alpha + \sin^2 \alpha \partial_\mu \Theta \partial^\mu \Theta \right. \\ & \left. + \sin^2 \alpha \sin^2 \Theta (\partial_\mu \Phi \partial^\mu \Phi - 2\mu_I \delta_{\mu 0} \partial^\mu \Phi) \right], \quad (11) \end{aligned}$$

which includes nonlinear couplings between the three fields. From Eq. (9) it is clear that the expansion of the term proportional to $\sin^2 \alpha$ produces an infinite number of charged pion self-interactions. The second Lagrangian contribution, \mathcal{L}_V , is related to the breaking of chiral symmetry. At a fundamental level it depends on quark interactions and masses. While \mathcal{L}_k is the only independent $O(p^2)$ Lagrangian that respects chiral symmetry, for the potential term there is no such restriction. In the following we will employ

$$\mathcal{L}_V = 2K \mu_I^2 \sin^2 \alpha \sin^2 \Theta + V, \quad (12)$$

where the first contribution on the rhs comes from the expansion of the first term in the round bracket of Eq. (1), while

$$V = K m_\pi^2 \text{Tr} (U + U^\dagger) = 4K m_\pi^2 \cos \alpha, \quad (13)$$

is the standard χ PT term giving masses to pions; an expression that can be immediately generalized to $SU(3)$ symmetry. From the above Lagrangian, one can obtain the free-energy density

$$F = F_K + F_V, \quad (14)$$

where

$$F_K = 2K \left[(\nabla \alpha)^2 + \sin^2 \alpha (\nabla \Theta)^2 + \sin^2 \alpha \sin^2 \Theta (\nabla \Phi)^2 \right], \quad (15)$$

contains the space derivatives, while

$$F_V = -2K \mu_I^2 \sin^2 \alpha \sin^2 \Theta + 4K m_\pi^2 (1 - \cos \alpha), \quad (16)$$

is the potential term; here we have appropriately added the vacuum free energy, $4K m_\pi^2$, so that F_V vanishes in the unbroken phase.

A. Homogeneous phase

We briefly recall the main properties of the homogeneous and static pion condensed phase in χ PT. In this case α, Φ and Θ are treated as variational parameters determined by minimizing the potential. Actually, F_V is independent of Φ , therefore this parameter cannot be fixed, while $\Theta = \pi/2$ minimizes F_V for any nonvanishing value of μ_I and α . As we have seen, this corresponds to a vanishing neutral pion component. Any isospin rotation $\Theta = \pi/2 + \delta\Theta$ would have a free-energy cost

$$\Delta F_V = 2K \mu_I^2 \sin^2 \alpha \sin^2 \delta\Theta, \quad (17)$$

and it is therefore energetically forbidden. The physical reason is that such rotation would imply that neutral pion states are populated, with a free-energy cost proportional to $\pi_0^2 = f_\pi^2 \cos^2 \Theta = f_\pi^2 \sin^2 \delta\Theta$ and the squared pion mass $m_\pi^2 \sim \mu_I^2$.

Upon substituting $\Theta = \pi/2$ in Eq. (16) we have that $F_V = -2K \mu_I^2 \sin^2 \alpha + 4K m_\pi^2 (1 - \cos \alpha)$ and then the free-energy minimum corresponds to

$$\alpha = \begin{cases} 0 & \text{for } |\mu_I| < m_\pi \\ \arccos\left(\frac{m_\pi}{\mu_I}\right) & \text{for } |\mu_I| \geq m_\pi, \end{cases} \quad (18)$$

therefore at $|\mu_I| = m_\pi$ the $U(1)$ subgroup generated by σ_3 is spontaneously broken and there is a second order phase transition from the naive vacuum to a BEC of charged pions. Since in the broken phase the free-energy minimum is attained for $\cos \alpha = m_\pi^2 / \mu_I^2$, it follows that any phase can be described taking $\alpha \in [0, \pi/2)$. For definiteness, hereafter we assume that $\mu_I \geq 0$.

Pressure and isospin number density in the broken phase are respectively given by

$$P = \frac{2K}{\mu_I^2} (\mu_I^2 - m_\pi^2)^2 \quad \text{and} \quad n_I = \frac{4K}{\mu_I^3} (\mu_I^4 - m_\pi^4), \quad (19)$$

where the pressure is clearly isotropic. Using the Gibbs-Duhem relation $\epsilon = \mu n - P$, we obtain the energy density

$$\epsilon = \frac{2K}{\mu_I^2} (\mu_I^2 - m_\pi^2) (\mu_I^2 + 3m_\pi^2), \quad (20)$$

and then the adiabatic speed of sound [42] by means of

$$c_s = \sqrt{\frac{\partial P}{\partial \epsilon}} = \sqrt{\frac{\mu_I^4 - m_\pi^4}{\mu_I^4 + 3m_\pi^4}}, \quad (21)$$

which is manifestly homogeneous and isotropic.

III. INHOMOGENEOUS PHASES

We now move to inhomogeneous pion systems using as guidance the information gathered in the previous analysis. As we have seen, the homogeneous phase free-energy

minimum is always attained when $\Theta = \pi/2$, corresponding to a vanishing neutral pion component. On the other hand, by changing the “control parameter” μ_I , the value of α that minimizes the free energy changes according to Eq. (18). Such variation, as a function of μ_I , is continuous. It thus appears natural to fix $\Theta = \pi/2$ and then look for possible inhomogeneous phases that could be realized by a space modulation of α . The free energy of the homogeneous ground state does not depend on Φ . The reason is that this field spans the flat direction of the potential and indeed the associated fluctuation is the Nambu-Goldstone boson. In general, space gradients of the phase are associated to a velocity field, for this reason we will assume that Φ is a space dependent field. This will allow us to consider vortices, characterized by a swirling velocity field.

To recap, we will assume that $\Theta = \pi/2$ and that both α and Φ are classical space-dependent fields. In this case,

the Lagrangian, see Eqs. (11) and (12), turns into

$$\mathcal{L} = 2K [\partial_\mu \alpha \partial^\mu \alpha + \sin^2 \alpha \partial_\mu \Phi \partial^\mu \Phi + 2m_\pi^2 (\cos \alpha - 1)] , \quad (22)$$

where we found convenient to replace $\Phi \rightarrow \Phi + \mu_I t$ to have a more compact expression. The free-energy contributions now read

$$F_K = 2K [(\nabla \alpha)^2 + \sin^2 \alpha (\nabla \Phi)^2] , \quad (23)$$

$$F_V = 2K [-\mu_I^2 \sin^2 \alpha + 2m_\pi^2 (1 - \cos \alpha)] , \quad (24)$$

and since we are interested in vortices, the natural ansatz is

$$\alpha = \alpha(x_1, x_2) , \quad \Phi = \Phi(x_1, x_2) , \quad (25)$$

where the indices 1, 2 indicate the two coordinates in the xy -plane; the vorticity is then expected to be along the z -direction.

We can now rewrite the gradients in Eq. (23) as follows:

$$(\partial_1 \alpha)^2 + (\partial_2 \alpha)^2 + \sin^2 \alpha [(\partial_1 \Phi)^2 + (\partial_2 \Phi)^2] = (\partial_1 \alpha \pm \sin \alpha \partial_2 \Phi)^2 + (\partial_2 \alpha \mp \sin \alpha \partial_1 \Phi)^2 \pm 2 \sin \alpha (\partial_1 \Phi \partial_2 \alpha - \partial_2 \Phi \partial_1 \alpha) , \quad (26)$$

where the last term on the rhs of the above expression has the following property:

$$\pm 2 \sin(\alpha) [(\partial_1 \Phi) (\partial_2 \alpha) - (\partial_2 \Phi) (\partial_1 \alpha)] dx_1 dx_2 = d\omega ,$$

with

$$\omega = \pm 2 \cos \alpha d\Phi , \quad (27)$$

a 1-form. If $\cos \alpha = 1$, then ω can be interpreted as the vorticity describing the spinning of the Φ field. Although in this case $d\omega = 0$, the circulation does not vanish if vortices are present. Similarly to what happens in the case of superconducting vortices in χ Pt, see [122], when $\cos \alpha \neq 1$, the obvious topological charge, $d\Phi$, is dressed by the background modulation. In the following we will take the positive sign in Eq. (27), and consider solutions with $\cos \alpha > 0$.

Upon substituting Eqs. (26) and (27) in the free-energy density in Eq. (23), we have that the total free energy satisfies the inequality

$$\mathcal{F} = \int_M dx_1 dx_2 F = \mathcal{F}_V + \mathcal{F}_K \geq 2K \int_M d\omega = 2K \int_{\partial M} \omega , \quad (28)$$

and therefore, when the free-energy potential vanishes, that is when

$$\int_M d^3x [-\mu_I^2 \sin^2 \alpha + 2m_\pi^2 (1 - \cos \alpha)] = 0 , \quad (29)$$

the total free energy equates \mathcal{F}_K . We will refer to this as the BPS condition. In addition, if the BPS equations

$$\partial_1 \alpha \pm \sin \alpha \partial_2 \Phi = 0 , \quad (30)$$

$$\partial_2 \alpha \mp \sin \alpha \partial_1 \Phi = 0 , \quad (31)$$

hold, the inequality in (28) is saturated, meaning that

$$\mathcal{F} = 2K \int_{\partial M} \omega , \quad (32)$$

therefore the free energy is completely determined by the behavior of vorticity at the boundary. This suggests, as we will see in the following, that it only depends on the boundary of the manifold and on the total winding number. Since the free energy is positive, vortex nucleation is not energetically favored. This happens because the system is not rotating, therefore there is no reason why a vortex should be nucleated. We will discuss the effect of rotation in Sec. VI. In numerical simulations with ultracold atoms adding a vortex to a static superfluid is usually obtained by the phase imprinting method. This procedure allows to scrutinize, among the possible vortex configurations, the one with the lowest free-energy cost.

We will explore such configurations employing the BPS condition, Eq. (29), which depends on the field α , the isospin chemical potential and the system size. On the other hand, the BPS equations (30) and (31) involve α and Φ . The set of equations (29), (30) and (31) can be solved using the following procedure. First, we find the solutions of the differential equations (30) and (31) using

appropriate boundary conditions. Then, we determine the constraint on μ_I and the system manifold to satisfy Eq. (29).

A. Boundary Conditions and vorticity quantization

For definiteness we assume that the system is in a cylinder of radius R and height ℓ_z . We consider flat space-time and we employ cylindrical coordinates

$$ds^2 = -dt^2 + dr^2 + r^2 d\varphi^2 + dz^2,$$

with r and φ the polar coordinates, while z is along the axis of the cylinder. The chiral field U in Eq. (4) must be single valued, therefore

$$U(r, \varphi) = U(r, \varphi + 2\pi), \quad (33)$$

and taking into account Eq. (5), with $\Theta = \pi/2$, we have that for any r ,

$$\alpha(r, \varphi) = \alpha(r, \varphi + 2\pi) + 2m\pi, \quad m \in \mathbb{Z} \quad (34)$$

$$\Phi(r, \varphi) = \Phi(r, \varphi + 2\pi) + 2n\pi, \quad n \in \mathbb{Z} \quad (35)$$

which imply that these fields are periodic functions of φ or are linearly dependent on it with integer slope. In configurations that are cylindrically symmetric only the latter is possible, indeed a modulation along the tangential direction would break the rotational invariance around the z -axis.

In presence of vortices, the condition in Eq. (35) with $n \neq 0$ appears natural taking into account that Φ is a phase. It implies that

$$\frac{1}{2\pi} \oint_{\Gamma_\infty} \nabla \Phi \cdot d\ell = n, \quad (36)$$

where Γ_∞ is the circle at spatial infinity and n is then the total winding number. If the cylindrical symmetry is broken, for instance by vortices not passing through the system center, then Φ becomes a combination of radial dependent functions and of sinusoidal functions of φ describing the winding around each vortex. Regarding the field α , it does not describe the phase of the condensate, but the modulation of its absolute value, see Eq. (9). In cylindrically symmetric configurations we expect that α describes the radial modulation of the condensate induced by the vortex. For noncentral vortices α will be as well a sinusoidal function of φ .

Regarding the vortex topological stability, given the translational invariance along the z -direction, the system is effectively in $2 + 1$ dimensional spacetime with a S^1 space boundary. For nonvanishing isospin chemical potential the pion system has only $U(1)$ internal symmetry, therefore the field boundary condition forms as well a circle S^1 . Thus, the map $S^1 \rightarrow S^1$ completely characterizes the behavior of the vortex at the boundary. Since this map cannot be smoothly deformed to the trivial map, it follows that the vortex solution is topologically stable.

B. Stress-energy tensor

The thermodynamic and mechanical properties of the system are determined by the the stress-energy tensor

$$T_\nu^\mu = \frac{\delta \mathcal{L}}{\delta \partial_\mu \alpha} \partial_\mu \alpha + \frac{\delta \mathcal{L}}{\delta \partial_\mu \Phi} \partial_\mu \Phi - \delta_\nu^\mu \mathcal{L}, \quad (37)$$

where we have assumed that the Θ field is fixed. It allows to obtain the energy density and pressure components, respectively given by

$$\epsilon = 2K \left[(\partial_r \alpha)^2 + \frac{1}{r^2} (\partial_\varphi \alpha)^2 + \sin^2 \alpha \left((\partial_r \Phi)^2 + \frac{1}{r^2} (\partial_\varphi \Phi)^2 \right) + \mu_I^2 \sin^2 \alpha - 2m_\pi^2 (\cos \alpha - 1) \right], \quad (38)$$

$$P_r = 2K \left[(\partial_r \alpha)^2 - \frac{1}{r^2} (\partial_\varphi \alpha)^2 + \sin^2 \alpha \left((\partial_r \Phi)^2 - \frac{1}{r^2} (\partial_\varphi \Phi)^2 \right) + \mu_I^2 \sin^2 \alpha + 2m_\pi^2 (\cos \alpha - 1) \right], \quad (39)$$

$$P_\varphi = 2K \left[-(\partial_r \alpha)^2 + \frac{1}{r^2} (\partial_\varphi \alpha)^2 - \sin^2 \alpha \left((\partial_r \Phi)^2 - \frac{1}{r^2} (\partial_\varphi \Phi)^2 \right) + \mu_I^2 \sin^2 \alpha + 2m_\pi^2 (\cos \alpha - 1) \right], \quad (40)$$

$$P_z = 2K \left[-(\partial_r \alpha)^2 - \frac{1}{r^2} (\partial_\varphi \alpha)^2 - \sin^2 \alpha \left((\partial_r \Phi)^2 + \frac{1}{r^2} (\partial_\varphi \Phi)^2 \right) + \mu_I^2 \sin^2 \alpha + 2m_\pi^2 (\cos \alpha - 1) \right], \quad (41)$$

where α and Φ are assumed to be functions of r and φ . Then, the isospin density

$$n_I = \frac{\partial P_r}{\partial \mu_I} = \frac{\partial P_\varphi}{\partial \mu_I} = \frac{\partial P_z}{\partial \mu_I} = 4K \mu_I \sin^2 \alpha, \quad (42)$$

depends only on α and it is in general space dependent. The stress-energy tensor has as well off-diagonal compo-

nents, in particular

$$T_{0\varphi} = \frac{4K}{r} \mu_I \sin^2 \alpha \partial_\varphi \Phi, \quad (43)$$

$$T_{0r} = 4K \mu_I \sin^2 \alpha \partial_r \Phi, \quad (44)$$

are the momentum densities in the xy -plane. The angular momentum with respect to the cylinder z -axis is given by

$$L_z = \int d^3r (\mathbf{r} \times \mathbf{T})_z, \quad (45)$$

where $\mathbf{T} = (T_{0r}, T_{0\varphi})$. For completeness,

$$T_{\varphi r} = \frac{4K}{r} [\partial_\varphi \alpha \partial_r \alpha + \sin^2 \alpha \partial_\varphi \Phi \partial_r \Phi], \quad (46)$$

is the shear stress, which should vanish because the system is not viscous: we are assuming negligible temperature.

IV. SINGLE VORTEX

We begin with the case of a single vortex imprinted to a non-rotating pion system. If the vortex is at the center of the system and it is parallel to the z -axis it does not break the cylindrical symmetry. In this case, the potential can only depend on the radial coordinate. Since the potential is a functional of α , it follows that we have to assume that

$$\alpha \equiv \alpha(r), \quad (47)$$

and thus the BPS Eqs. (30) and (31) read

$$\partial_r \alpha \pm \sin \alpha \frac{1}{r} \partial_\varphi \Phi = 0, \quad (48)$$

$$\sin \alpha \partial_r \Phi = 0, \quad (49)$$

where the latter equation implies that $\Phi \equiv \Phi(\varphi)$. Given the periodicity condition in Eq. (35), as we already discussed, there are two different class of solutions: Φ is a sinusoidal function of φ or it is linearly depend on it. The sinusoidal angular dependence is incompatible with Eq. (48), because α does not depend on φ . For this reason we can only consider solutions of Eq. (49) of the form

$$\Phi = n \varphi, \quad (50)$$

where $n \in \mathbb{Z}$ is the winding number. In this way we have that Eq. (48) turns into

$$\frac{d\alpha}{dr} + \frac{n}{r} \sin \alpha = 0, \quad (51)$$

where we restrict to consider the positive sign because n can be a positive or negative integer. The above equation is invariant under the scaling $r \rightarrow \lambda r$, with λ a constant, it is indeed independent of all the energy scales m_π , μ_I and f_π . It has no information on interactions and masses because it is solely determined by the derivative term.

The solution of the differential equation (51) is

$$\alpha(r) = 2 \arctan(C^n r^{-n}), \quad (52)$$

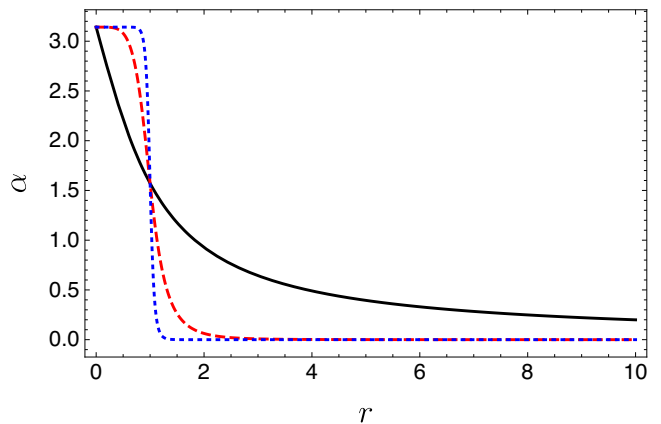


FIG. 1. Modulation of the α function determined by a single vortex at the center, see Eq. (52), as a function of the distance from the z -axis of the cylinder (in units of $1/m_\pi$). The reported results are obtained with winding number $n = 1$, solid black line, $n = 5$, dashed red line and $n = 20$, dotted blue line. All the lines intersect at $r = 1, \alpha = \pi/4$.

which depends on the integration constant, C , that determines the typical length scale variation of α . In the following we will set $C = 1/m_\pi$, and thus all length scales will be expressed in units of $1/m_\pi$. Although arbitrary, this is somehow a natural choice, given that in the leading order χ PT Lagrangian f_π factorizes and $\mu_I \sim m_\pi$. In Fig. 1, we report the behavior obtained with $n = 1$, $n = 5$ and $n = 20$. All the lines start from $\alpha = \pi$ for $r = 0$, intersect at $r = 1, \alpha = \pi/2$, and tend to 0 for large r . With increasing n , the variation of α around $r = 1$ is more pronounced, indeed it tends to the Heaviside step function $\Theta_H(1 - r)$ for $n \rightarrow \infty$. The region $r < 1$ corresponds to momenta larger than m_π meaning that the used leading order χ PT Lagrangian is not adequate to describe it. This is also signaled by the fact that in the homogeneous phase we have seen that $\alpha \in [0, \pi/2)$, in that case values of α larger than $\pi/2$ correspond to imaginary isospin chemical potentials.

Upon substituting Eqs. (50) and (51) in Eqs. (38), (39), (40) and (41), the energy density and pressure components are respectively given by

$$\begin{aligned} \epsilon &= 2K \left[\sin^2 \alpha \left(\mu_I^2 + \frac{2n^2}{r^2} \right) - 2m_\pi^2 (\cos \alpha - 1) \right], \\ P_r = P_\varphi &= 2K \left[\mu_I^2 \sin^2 \alpha + 2m_\pi^2 (\cos \alpha - 1) \right], \\ P_z &= 2K \left[\left(\mu_I^2 - \frac{2n^2}{r^2} \right) \sin^2 \alpha + 2m_\pi^2 (\cos \alpha - 1) \right], \end{aligned} \quad (53)$$

meaning that the pressure is isotropic in the xy -plane.

The isospin number density in Eq. (42) takes the expression

$$n_I = 4K \mu_I \sin^2 \alpha = 16K \mu_I \frac{r^{2n}}{(1 + r^{2n})^2}, \quad (54)$$

which is invariant under $n \rightarrow -n$; in other words, the vortex and the anti-vortex solutions are both independent

of φ and have the same radial dependence. The isospin number density vanishes at large distances as r^{2n} . This behavior is determined by the fact that α tends to 0 for large values of r . Notice that it is not possible to consider a vortex as a perturbation of a homogeneous background: the number density is completely determined by the vortex. A homogeneous background corresponds to α constant, thus to consider a vortex on top of it one should replace $\alpha \rightarrow \alpha + A$, where A is some constant. However, the only solution compatible with the BPS Eq. (51) is the one with $A = 0$.

Regarding the off-diagonal elements of the stress-energy tensor, the shear stress in Eq. (46) vanishes, therefore the system is inviscid. The component T_{0r} in Eq. (44) vanishes as well, meaning that there is no radial flow, while from Eq. (43) we have that

$$T_{0\varphi} = n \frac{4K}{r} \mu_I \sin^2 \alpha = n \frac{n_I}{r}, \quad (55)$$

which corresponds to the momentum density along the tangential direction. These results imply that the pion gas is spinning with tangential velocity $v_\varphi \propto 1/r$ as appropriate for a quantized vortex in a superfluid. From Eq. (55) we can calculate the angular momentum along the z -axis, which is given by

$$L_z = \int d^3x T_{0\varphi} r = n N_I, \quad (56)$$

where

$$N_I = \int d^3x n_I, \quad (57)$$

is the total isospin number. In other words, the angular momentum per particle is \hbar as in standard superfluids.

A. Global BPS condition

The components of the stress-energy tensor depend on μ_I , which cannot take arbitrary values. The reason is that we are asking that the BPS condition in Eq. (29) be satisfied. Considering a vortex at the center of the cylinder and assuming a constant isospin chemical potential, we obtain that

$$\mu_I^2 = 2m_\pi^2 \frac{\int_0^R dr r (1 - \cos \alpha)}{\int_0^R dr r \sin^2 \alpha}, \quad (58)$$

which implies that μ_I depends on the behavior of the condensate across the whole system. We shall refer to equations like (58) as global BPS conditions. It is important to remark that this means that the system is not at a stationary point of the action, therefore Eqs. (50) and (51) are not in general a solution of the Euler-Lagrange equations obtained from the Lagrangian in Eq. (22). Although corresponding to an unstable configuration, we

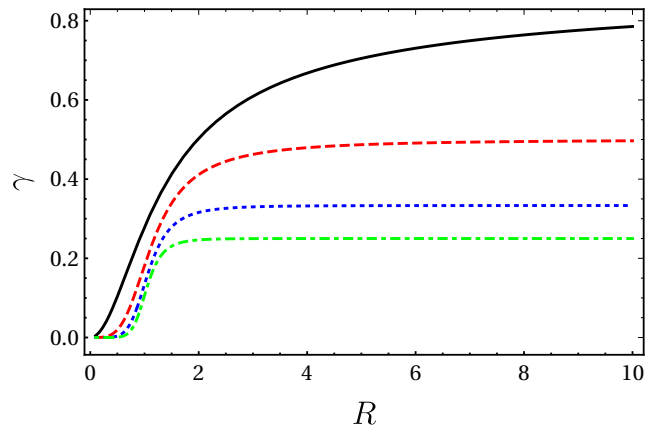


FIG. 2. Values of $\gamma = m_\pi^2/\mu_I^2$ that satisfy the global BPS condition, see Eq. (58), as a function of the distance from the z -axis of the cylinder (in units of $1/m_\pi$). The reported results are obtained with winding number $n = 1$, solid black line, $n = 2$, dashed red line, $n = 3$, dotted blue line, and $n = 4$, dot-dashed green line.

find instructive this case: as we will see, it has some interesting features.

Let us consider a central vortex with minimal nontrivial winding $n = 1$. Using Eq. (52) we have that

$$\int_0^R dr r \sin^2 \alpha = 2 \left[-\frac{R^2}{1+R^2} + \log(1+R^2) \right], \quad (59)$$

while

$$\int_0^R dr r (1 - \cos \alpha) = \log(1+R^2), \quad (60)$$

therefore we obtain the analytical expression

$$\gamma(R) = \frac{m_\pi^2}{\mu_I^2} = 1 - \frac{R^2}{1+R^2} \frac{1}{\log(1+R^2)}, \quad (61)$$

corresponding to the solid black line in Fig. 2. This function logarithmically converges to 1 from below. This means that for any dimension of the system, it exists a value $\mu_I > m_\pi$ that allows to satisfy the global BPS condition. In the homogeneous phase we found that values of μ_I larger than m_π indicate pion condensation, with α given in Eq. (18). Here, there is a modulation of α , however in the thermodynamic limit $R \rightarrow \infty$, such modulation, for $r > 1$, smoothens and at the same time we have that $\mu_I \rightarrow m_\pi$. This suggests that for $\mu_I \gtrsim m_\pi$, the global BPS condition approximates the actual stationary point of the action. The above reasoning can be extended to arbitrary winding number. In particular, a vortex at the center of the system with arbitrary winding number, n , satisfies the global BPS condition if $\gamma \leq 1/n$, as shown in Fig. 2. In other words, the vortex solution with winding number n satisfying the global BPS condition can only appear for $\mu_I \geq \sqrt{n} m_\pi$.

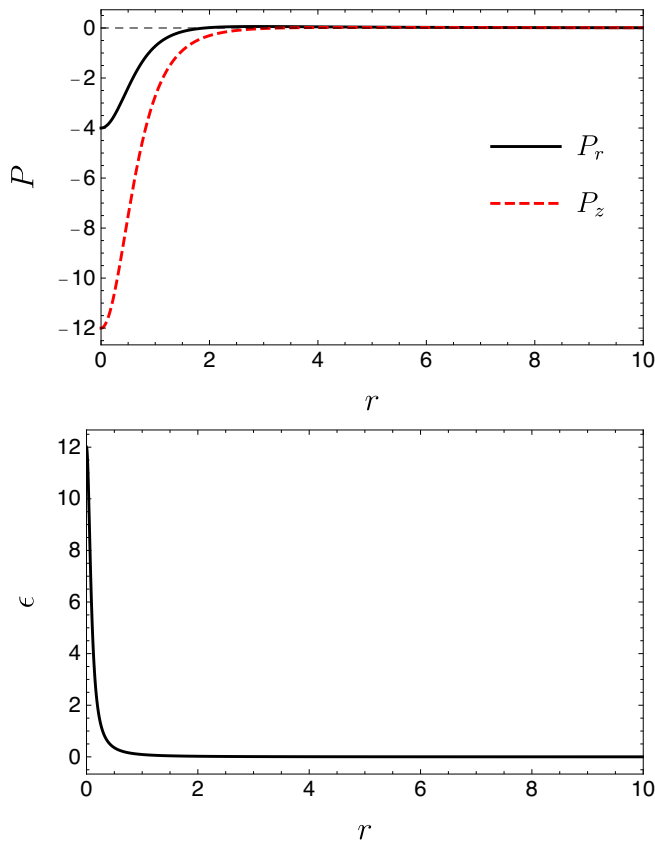


FIG. 3. Pressure and energy density determined by a central vortex with winding number $n = 1$ (in units of $2Km_\pi^2$), as a function of the distance from the z -axis of the cylinder (in units of $1/m_\pi$). The results are obtained using the global BPS condition, see Eqs. (58) and (61) with $R = 10$. Top panel the pressure in the xy -plane is in black, while the pressure along the z -direction is the dashed red line. Bottom panel, energy density.

Once the isospin chemical potential is known, we can compute the various thermodynamic quantities. We report in Fig. 3 pressure (top panel) and energy density (bottom panel) for the case $n = 1$ and $R = 10$. Results obtained with different values of R are similar. Both pressure components are negative at small distance from the cylinder axis, while they become positive at sufficiently large distances. The pressure along z vanishes at $r \simeq 3.3$, while the pressure in the xy -plane vanishes at $r \simeq 1.9$. These values slightly increase with the system size R . Negative values of the pressure are typical of vortices: high fluid velocity produces a local depression. The negative pressure in xy -plane indicates that the vortex is willing to capture matter, the system is therefore unstable unless some external force will prevent matter from falling in the vortex. Such behavior is a consequence of the fact that the considered solutions of the BPS equations (58) do not correspond to an action stationary state. Negative values of the pressure in the z -direction are instead due to the vortex swirling: as

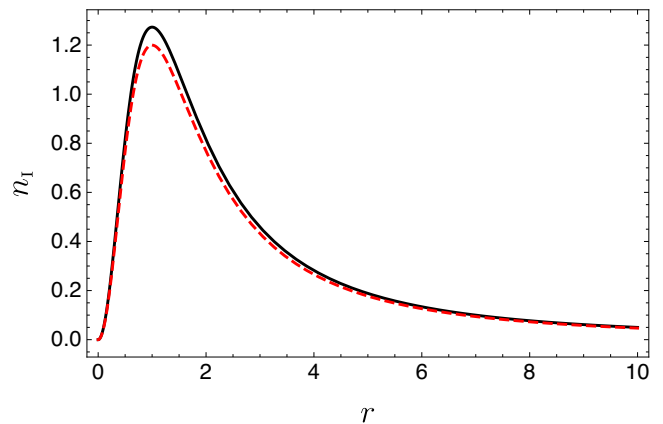


FIG. 4. Radial dependence of the isospin number density for vortices with winding number $n = 1$, $R = 10$ (solid black) and $R = 20$ (dashed red) normalized to $16K\mu_I$. Distances are in units of $1/m_\pi$.

in standard vortices the pressure along the vortex axis becomes large and negative close the core.

Negative values of the pressure close to the vortex suggest an interpretation in terms of a space dependent bag. As in the MIT bag model, the negative pressure may serve to confine matter: pions cannot spread from the vortex. For each value of r , the pressure is constant that is independent of φ and z . This means that there is a sort of cylindrical confinement. In the MIT bag model the bag pressure is about $(140 - 150 \text{ MeV})^4$, here we find that it is of the order of $16Km_\pi^2 = 4f_\pi^2 m_\pi^2 \simeq m_\pi^4$, and thus of a similar magnitude. As in the MIT bag model, this negative pressure comes with a positive energy density, see the bottom panel in Fig. 3. Moreover, both pressure and energy density tend to vanish for large r , meaning that confinement becomes negligible far from the place where the number density is large. The number density is indeed peaked at $r = 1/\sqrt{2}$, as can be seen from Fig. 4, where we report n_I for two different values of the radial size. Such behavior of the number density is somehow similar to that of trapped ultracold atoms: the vortex core does indeed correspond to the region where the condensate vanishes, while the trapping potential induces a vanishing number density at the edge of the system. Here we observe a similar behavior, but the decrease of the number density far from the vortex core is not due to an external potential: it is a consequence of pion self-interactions. The expression of the number density comes from the term proportional to $\sin^2 \alpha$ in the Lagrangian. At sufficiently large distances from the vortex core $\alpha \ll 1$, see Fig. 1, and we can Taylor expand the sine function. Taking into account Eq. (9) we can interpret the sinusoidal terms in α as a series of pion self-interactions which become more and more relevant as one approaches a vortex from large r . As already noticed, this calls for adding more terms to the χ PT Lagrangian to describe the short distance behavior close to the vor-

tex core. Combining Eq. (61) with Eqs. (42) and (57) we find that the total isospin number is given by

$$N_I = \frac{16K\pi\ell_z}{m_\pi^2\sqrt{\gamma(R)}} \left(\log[1+R^2] - \frac{R^2}{1+R^2} \right), \quad (62)$$

where ℓ_z is the transverse dimension of the system measured in units of $1/m_\pi$. Since Eq. (56) holds, this is as well the total angular momentum.

B. Local BPS condition

In the homogeneous phase, α and μ_I are linked by Eq. (18). In a system in which μ_I is a smooth function of r , one expects that α is modulated as well. Conversely, a space modulation of α should go along with a space modulation of μ_I . Considering a space dependent isospin chemical potential allows us as well to overcome the main limitation of the global BPS condition: Eq. (58) ensures that the free-energy contribution of the potential term vanishes, but it does not correspond to a stationary point of the action. We can define a local BPS condition such that the free energy vanishes at every point. This happens if the isospin chemical potential is space dependent and takes the expression

$$\mu_I^2 = 2m_\pi^2 \frac{1 - \cos \alpha}{\sin^2 \alpha}, \quad (63)$$

such that $F_V = 0$ at every point. In this case the solutions of the BPS equations are as well solutions of the Euler-Lagrange equations,

$$\sin^2 \alpha \partial^\mu \partial_\mu \Phi + \sin(2\alpha) \partial_\mu \alpha \partial^\mu \Phi = 0, \quad (64)$$

$$\partial_\mu \partial^\mu \alpha - \sin \alpha \cos \alpha \partial_\mu \Phi \partial^\mu \Phi = 0, \quad (65)$$

the system is indeed at an action stationary point. Although general, this result can be easily shown for a single vortex at the center. Regarding Eq. (64), since $\alpha \equiv \alpha(r)$ and $\Phi \equiv \Phi(\varphi)$ it follows that $\partial_\mu \alpha \partial^\mu \Phi = 0$. Given Eq. (50), we also have $\partial^\mu \partial_\mu \Phi = 0$, therefore Eq. (64) is satisfied. Regarding Eq. (65), substituting Eq. (50), we have that

$$\nabla^2 \alpha = \frac{n^2}{r^2} \sin \alpha \cos \alpha, \quad (66)$$

which can be proven to be satisfied by the BPS solution by repeatedly differentiating Eq. (51); in this way we obtain that

$$\nabla^2 \alpha = -n \frac{1}{r} \partial_r \sin \alpha = -n \frac{1}{r} \cos \alpha \partial_r \alpha = \frac{n^2}{r^2} \sin \alpha \cos \alpha, \quad (67)$$

which indeed agrees with (66). Therefore, the BPS solution in Eqs. (50) and (52) are solutions of the Euler-Lagrange equations.

Taking into account Eq. (72) we have that

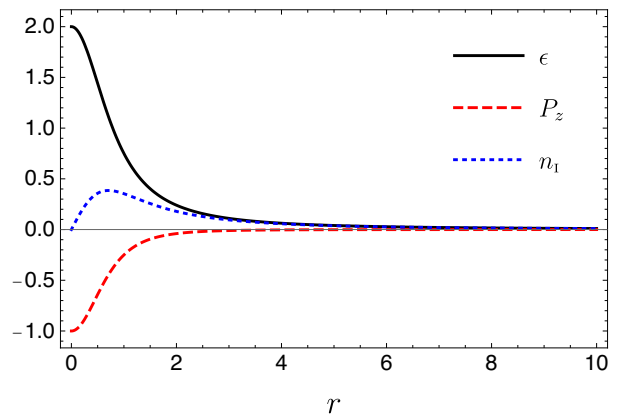


FIG. 5. Radial dependence of the energy density, pressure (in units of $16Km_\pi^2$) and number density (in units of $16Km_\pi$). Results obtained with a central vortex with winding number $n = 1$ using the local BPS condition, see the main text for more details. Distances are in units of $1/m_\pi$.

$$\mu_I^2 = m_\pi^2 \left(1 + \frac{1}{r^{2n}} \right), \quad (68)$$

therefore it diverges at the vortex center. However, as already noticed, the used χ PT leading order Lagrangian is valid for chemical potentials not much larger than the pion mass. For this reason we assume that the above solution is valid only for $r \geq 1$, corresponding to $\mu_I \leq \sqrt{2}m_\pi$. The inclusion of higher order terms in the χ PT Lagrangian should regularize of the vortex core.

From Eq. (63), we have that

$$\alpha = 2 \arctan \left(\sqrt{\frac{\mu_I^2}{m_\pi^2} - 1} \right), \quad (69)$$

which can be seen as a combination of the local BPS condition with the BPS solution in Eq. (52). Upon substituting these expressions in Eq. (53), we obtain that

$$\begin{aligned} \epsilon &= 16Km_\pi^2 \frac{2+r^2}{(1+r^2)^2}, \\ P_r &= P_\varphi = 0, \\ P_z &= -16Km_\pi^2 \frac{1}{(1+r^2)^2}, \\ n_I &= 16Km_\pi \frac{r}{(1+r^2)^{3/2}}, \end{aligned} \quad (70)$$

therefore the pressure in the xy -plane is isotropic, homogeneous and equates the vacuum pressure. In Fig. 5 we show the radial dependence of ϵ (black solid line), n_I (dotted blue line) and P_z (dashed red line). Note that n_I is peaked at short distance from the vortex core, therefore the sort of confinement effect found using the global BPS condition still holds. Since the pressure in the xy -plane vanishes, the vortex does not tend to accrete pions

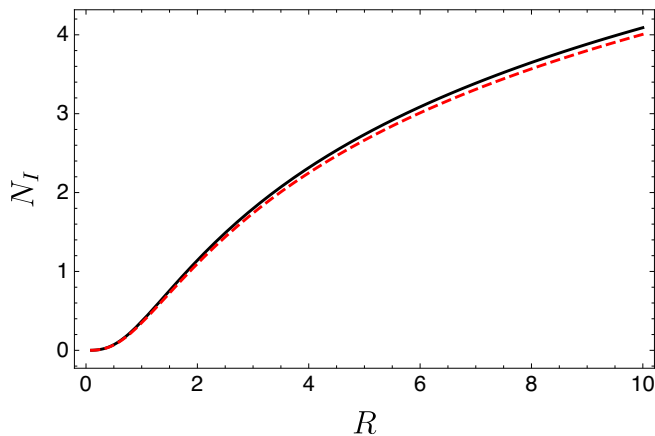


FIG. 6. Total isospin number in presence of a central vortex as a function of the cylinder radius, R . The isospin number is in units of $16\pi\ell_z K/m_\pi^2$, while the radius is in units of $1/m_\pi$. The solid black line is obtained with the global BPS condition, while the dashed red line using the local BPS condition.

from the surrounding medium and it is therefore stable. Although we are considering a stationary point of the action, P_z is negative. As already observed, this is a typical effect due to the vortex swirling. In agreement with the results obtained using the global BPS case, we checked that the viscous component vanishes, that is $T_{r\varphi} = 0$.

The angular momentum takes the same expression reported in Eq. (56), that is $L_z = nN_I$, but now the total number of particles is given by

$$N_I = \int d^3x n_I = \frac{32\pi K \ell_z}{m_\pi^2} \left(\operatorname{arcsinh}(R) - \frac{R}{\sqrt{1+R^2}} \right), \quad (71)$$

that is a positive and monotone function of R . In Fig. 6, we compare the total isospin number obtained with the global (solid black) and local (dashed red) BPS conditions. The two lines are very similar because in both cases the dominant contribution comes from the derivative part of the Lagrangian.

V. MORE GENERAL VORTEX CONFIGURATIONS

The previously obtained results can be extended to more general vortex configurations. We first consider a noncentral vortex and then the most general case of an arbitrary number of vortices.

A. Noncentral vortex

When the vortex is not at the center of the system the cylindrical symmetry is broken. However, one can generalize the central vortex solution by taking

$$\alpha = 2 \arctan(|\mathbf{r} - \mathbf{r}_v|^{-n}), \quad (72)$$

and

$$\Phi = n \arctan\left(\frac{y - y_v}{x - x_v}\right), \quad (73)$$

where $\mathbf{r}_v = (x_v, y_v) = r_v(\cos \varphi_v, \sin \varphi_v)$ is the vortex position and n its winding number. Upon substituting these expressions in Eq. (29), the global BPS condition is satisfied when

$$\gamma(R, r_v) = \frac{-R^2 - \chi + \chi \log\left(\frac{r_v^2(R^2 - r_v^2 + 1 + \chi)}{-R^2 + r_v^2 - 1 + \chi}\right) + r_v^2 + 1}{\chi \log\left(\frac{r_v^2(R^2 - r_v^2 + 1 + \chi)}{-R^2 + r_v^2 - 1 + \chi}\right)}, \quad (74)$$

where

$$\chi(R, r_v) = \sqrt{R^4 - 2R^2(r_v^2 - 1) + (r_v^2 + 1)^2}. \quad (75)$$

This result is independent of the polar position of the vortex, as expected. In the limit $r_v \rightarrow 0$, the central vortex result in Eq. (61) is recovered. Regarding the local BPS condition, the space dependent isospin chemical potential is obtained substituting Eq. (72) in Eq. (63). This ensures that $F_V = 0$ at every point.

The two BPS conditions give similar results as is evident in Fig. 7, where we show the dependence of the angular momentum on the distance of the vortex from the z -axis. The two lines correspond to the results obtained with the global (solid black) and local (dashed red) BPS conditions. Quite remarkable is the fact that the angular momentum changes sign if the vortex is very close to the boundary. This effect depends on the peculiar isospin number density produced by a vortex, which is peaked in a region close to the vortex and vanishes both at the vortex core and far from it. When the vortex approaches the boundary, a large fraction of pions rotates clockwise giving a negative contribution to the angular momentum. The angular momentum reduction close to the boundary is observed as well in systems of superfluid ultracold atoms. However, in that case the angular momentum vanishes without changing sign when the vortex reaches the boundary.

B. Multi-vortex configurations

The single noncentral vortex solution in Eqs. (72) and (73) can be extended to multi-vortex configurations. To this end, we rewrite the BPS equations (30) and (31) as

$$\partial_2 \Phi = \mp \frac{\partial_1 \alpha}{\sin \alpha}, \quad \partial_1 \Phi = \pm \frac{\partial_2 \alpha}{\sin \alpha}, \quad (76)$$

differentiating the first equation by ∂_1 , the second by ∂_2 and combining them one arrives at the following nonlinear differential equation

$$\nabla^2 \alpha - \cot \alpha (\nabla \alpha)^2 = 0, \quad (77)$$

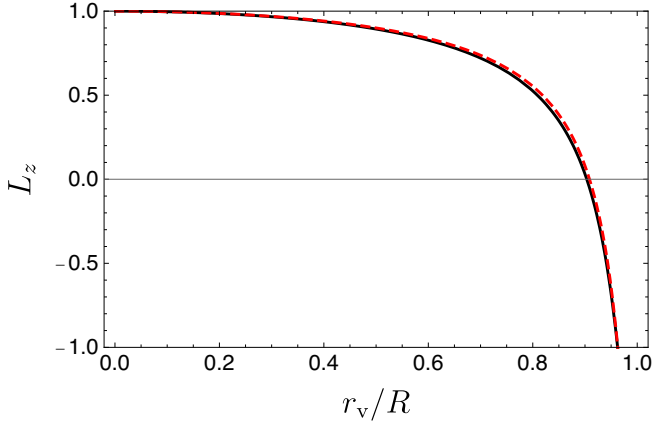


FIG. 7. Angular momentum generated by a single vortex at a distance r_v from the z -axis of the cylinder. The solid black line refers to the results obtained with the global BPS condition, while the dashed red line is obtained using the local BPS condition.

which by means of the change of variable

$$\alpha = 2 \arctan(\exp X), \quad (78)$$

can be rewritten as

$$\sin \alpha \nabla^2 X = 0. \quad (79)$$

Since at the BPS point α does not identically vanish, Eq. (77) is *exactly equivalent* to the Laplace's equation

$$\nabla^2 X = 0, \quad (80)$$

while (76) turns into

$$\partial_2 \Phi = \mp \partial_1 X, \quad \partial_1 \Phi = \pm \partial_2 X, \quad (81)$$

meaning that X and Φ are two conjugated harmonic functions. At the center of a vortex, $\alpha = \pi$, see Fig. 1, thus from Eq. (78) it follows that X is singular. In two dimensions, the most general harmonic function with singularities is the Green function

$$X = - \sum_j^N n_j \log(|\mathbf{r} - \mathbf{r}_j|), \quad (82)$$

where N is the number of vortices, while $\mathbf{r}_j = (x_j, y_j)$ and n_j are respectively the position in the xy -plane and winding number of the j -th vortex. From Eq. (78) we then obtain

$$\alpha = 2 \arctan \left(\prod_{j=1}^N |\mathbf{r} - \mathbf{r}_j|^{-n_j} \right), \quad (83)$$

while from Eq. (81) we find

$$\Phi = \sum_j^N n_j \arctan \left(\frac{y - y_j}{x - x_j} \right), \quad (84)$$

which generalize the previously found single vortex solution Eqs. (72) and (73). These equations have several interesting features: Eq. (84) coincides with the Feynman-Onsager ansatz for the phase of superfluid multi-vortex configurations, see [115, 133] and references therein. Even if there are many vortices with arbitrary winding number, thus making X large in absolute value, α will always be in the $(0, \pi]$ interval. Moreover, despite the highly non-linear interactions present in χ PT, the BPS point manifests a linear composition law. The reason is that X satisfies the Laplace equation (80), thus given an arbitrary number of solutions, their linear combination is still a solution. In particular, if

$$X_1 = \sum_j^{N_1} n_j \log(|\mathbf{r} - \mathbf{r}_j|), \quad (85)$$

$$X_2 = \sum_k^{N_2} n_k \log(|\mathbf{r} - \mathbf{r}_k|), \quad (86)$$

are two solutions of the Laplace equation, then $\alpha_{1,2} = 2 \arctan(\exp X_{1,2})$ are two solutions of Eq. (77) with N_1 and N_2 vortices, respectively. Then, their non-linear combination

$$\begin{aligned} \alpha_{1 \oplus 2} &= 2 \arctan(\exp(aX_1 + bX_2)) \\ &= 2 \arctan \left(\prod_{j=1}^{N_1} |\mathbf{r} - \mathbf{r}_j|^{-2an_j} \prod_{k=1}^{N_2} |\mathbf{r} - \mathbf{r}_k|^{-2bn_k} \right) \\ &= 2 \arctan \left(\prod_{l=1}^N |\mathbf{r} - \mathbf{r}_j|^{-2n_l} \right), \end{aligned} \quad (87)$$

and

$$\Phi_{1 \oplus 2} = \sum_l^N n_l \arctan \left(\frac{y - y_l}{x - x_l} \right), \quad (88)$$

are still valid solutions with $N = N_1 + N_2$ vortices having winding numbers $n_l = an_j$ for $l \leq N_1$ and $n_l = bn_k$ for $N_1 < l \leq N_2$. Imposing the periodic boundary conditions in Eqs. (34) and (35), only integer values of a and b result admissible.

VI. FREE ENERGY AND CRITICAL ROTATION FREQUENCY

At the BPS point the system is not sensitive to the actual form of the potential, because the contribution of the potential free energy by definition vanishes. This means that the free energy can only depend on the geometry and topology of the system, in other words the system size and winding number.

The free energy for a configuration of one single vortex at the center has the analytical expression

$$\mathcal{F} = n \frac{8\pi K \ell_z}{m_\pi} \frac{R^2}{1 + R^2}, \quad (89)$$

which is obtained combining Eqs. (23), (50) and (52). This result differs significantly from the standard, approximate expression obtained in superfluids [116]. In that case the free energy diverges logarithmically with R and scales with n^2 . Here the free energy is bounded: at most it takes the value $\mathcal{F}_{\max} = n 8\pi K \ell_z / m_\pi$. This happens because the number density vanishes at large distances. More precisely, the free energy is dominated by the kinetic energy of a vortex, which can be written as

$$E_k \sim \frac{1}{2} \ell_z \int_0^{2\pi} d\varphi \int_0^R r dr \rho v_s^2, \quad (90)$$

where ρ is the mass density and

$$v_s \propto \frac{n}{r}, \quad (91)$$

is the superfluid velocity. In standard superfluids, far from a vortex ρ tends to a constant value, thus the above integral yields

$$E_k \sim n^2 \log(R), \quad (92)$$

it is therefore logarithmically divergent and scales with n^2 . In the present case the kinetic energy tends to a constant value at large R because the isospin number density at large distances scales as $1/r^{2n}$, see Eq. (54), and then the integral in Eq. (90) becomes convergent. The linear scaling with the winding number is instead due to the fact that $\rho \sim n_I \sim r^{2n}/(1+r^{2n})^2$, defining $x = r^n$, one immediately finds that

$$\frac{dr}{r} = \frac{1}{n} \frac{dx}{x}, \quad (93)$$

and then substituting this expression in Eq. (90) and taking into account Eq. (91) it follows that the energy cost of a vortex scales with n . This means that vortices with high winding number are not energetically unstable. Thinking of such configurations as made of n overlapping vortices, each of them with winding number 1, the free-energy cost linearly scales with the number of vortices, as if they were not interacting. Upon substituting Eqs. (83) and (84) in Eq. (15) we have numerically verified this aspect computing the free energy of many vortices as a function of their relative distance. We find that configurations of n vortices, all of them sufficiently close to the center, have the same free energy of a single vortex with winding number n . This is the analogous of the behavior found in superconducting vortices at the critical point where type II superconductors turn into type I superconductors [134].

Given the symmetry of the system, the free energy of a vortex depends only on its radial distance from the center. We show in Fig. 8 the free energy of a vortex at a distance r_v from the axis of the cylinder, normalized to the value it takes when the vortex is at the center. When the vortex is close to the center, its free energy is independent of its radial position. A vortex feels the

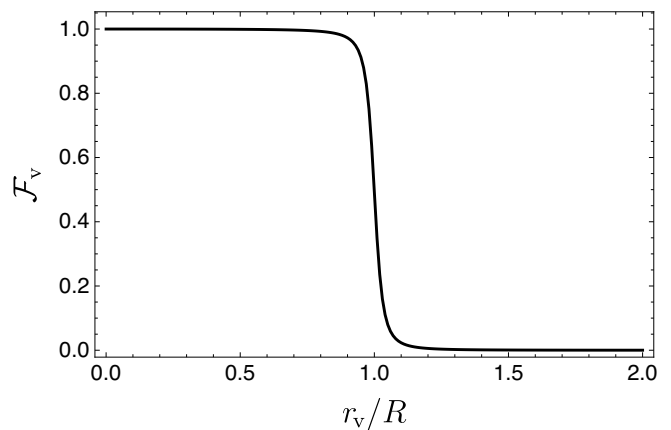


FIG. 8. Dependence of the single vortex free energy as a function of its radial position. The free energy has been normalized to its value when the vortex is at the center, see Eq. (89).

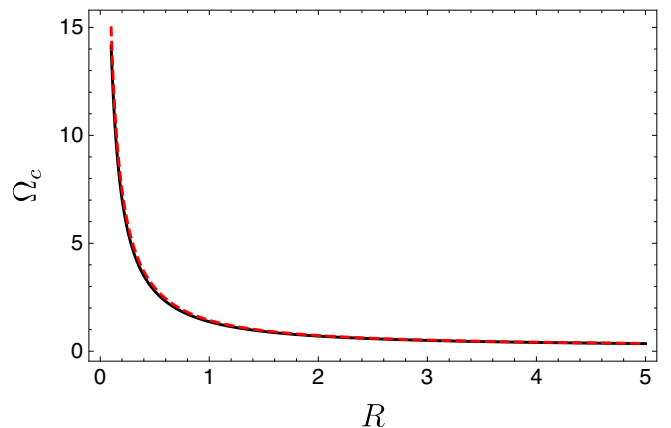


FIG. 9. Estimated critical frequency, in units of m_π , for cylindrical systems of different radii (in units of $1/m_\pi$). The black line is obtained using the global BPS condition, while the dashed red line with the local BPS condition.

boundary only when it is close to it, then for $r_v = R$ its free energy becomes approximately one half of the value in Eq. (89). In summary, the free-energy cost of each vortex does not depend on the presence of other vortices but only on its proximity to the boundary.

The expression in Eq. (89) allows us to estimate the critical frequency necessary for vortex nucleation. Suppose that the system is in a container rotating at an externally imposed rotation frequency Ω . If the system is superfluid, there should exist a critical rotation frequency, Ω_C , for vortex nucleation. We estimate it by the balance between the vortex energetic cost, as evaluated above, and the kinetic energy gain occurring when the superfluid co-rotates with the container. This means that there is an additional free-energy contribution, not included in the above analysis. Considering the frame rotating at the externally imposed rotation frequency, the

total free energy is

$$\mathcal{F}_{\text{tot}} \simeq \mathcal{F} - \Omega L_z, \quad (94)$$

where \mathcal{F} is given in Eq. (89). This is an approximate expression because we have evaluated the free-energy cost of a vortex in a nonrotating superfluid and then added the free-energy gain associated to rotation. In principle, one should evaluate \mathcal{F}_{tot} starting from the χ PT Lagrangian in a rotating frame; we will discuss this topic in a future publication. In the present paper we content ourselves with the approximate expression in Eq. (94). The condition of vortex nucleation at the trap center is then $\mathcal{F}_{\text{tot}} = 0$, which gives

$$\Omega_c = \frac{\mathcal{F}}{L_z} = \frac{\mathcal{F}}{N_I}, \quad (95)$$

where the total isospin number is in Eq. (62) for the global BPS condition and in Eq. (71) for the local BPS condition. In this approximation the critical frequency is proportional to m_π and scales with R as shown in Fig. 9. The critical frequency obtained with the global BPS condition almost matches that obtained with the local BPS condition because the free energy takes the same value in the two cases and the total isospin numbers are very similar, see Fig. 6. For a more realistic estimate of the critical frequency one should also take into account that vortices are typically generated at the boundary of the system. Given the radial dependence of the angular momentum reported in Fig. 7, dynamical vortex nucleation at the boundary is energetically disfavored because L_z is negative, meaning that the contribution ΩL_z in Eq. (94) is positive: it is a free-energy cost. Presumably, if a vortex is dynamically nucleated at the boundary, it will rapidly move towards the center of the system: in this way L_z becomes large and positive, hence minimizing the total free energy.

VII. CONCLUSION

We have analyzed the possible existence of quantized vortices in the pion condensed phase. Our main investigation tool has been leading order χ PT combined with the BPS critical condition. This method is expected to be valid for isospin chemical potentials close to the pion mass. Actually, the BPS critical point is realized by appropriately tuning the isospin chemical potential and the system size. For definiteness we have assumed that the system has cylindrical symmetry, eventually broken by noncentral vortices. This makes it similar to those realized in ultracold atom systems. However, in this case, pions are self-confined by the vortex: the number density peaks in a region close to the vortex and tends to vanish both at the vortex core and at the boundary. This suggests that the actual geometrical realization of the system is immaterial insofar the vortex is sufficiently far from the boundary.

Single vortex as well as multi-vortex states with quantized vorticity have been obtained. We have analyzed the single BPS vortex in detail. In particular, we have computed exactly the corresponding energy density and momentum fluxes as well as the quantized angular momentum. The existence of quantized vortices, as well as the vanishing of dissipative terms in the stress-energy tensor, unambiguously imply that the pion condensed phase is superfluid. In addition, we found that at the BPS point the free energy is bounded and it linearly scales with the winding number. Therefore, vortices with large winding number are not unstable. Such a result is expected to change when perturbations to the BPS equations are included. This should allow us to check whether the obtained stationary solutions correspond to minima of the free energy. Work in this direction is underway.

The obtained results can in principle be tested by LQCD simulations in rotating frames [135]. We are not aware of any such simulation at nonvanishing μ_I . By appropriately tuning the isospin chemical potential, vortices should appear close to the second order phase transition. Vortex nucleation at the boundary of these systems should happen as in standard superfluids, then followed by a rapid vortex drift towards the center of the cylinder. If doable, these simulations would be of the great interest, because could indicate the possible generation of vortices of self-confined pions as well as the existence of other interesting effects triggered by rotation [136–138].

Whether our results could be relevant in astrophysics is an open question. Pion stars [42, 83, 139–143] or neutron stars with pion condensation in the core [28, 144] could be two types of compact objects produced during the collapse of massive stars. Such exotic compact stars are expected to rapidly cool and spin at high frequency, hosting a large number of superfluid vortices. As we have shown, pion vortices have large effect on the isospin number density, therefore they could modify the stellar structure.

VIII. ACKNOWLEDGMENTS

F.C. has been funded by Fondecyt grants No. 1240048, 1240043, 1240247 and by Grant ANID EXPLORACIÓN 13250014. The Centro de Estudios Científicos (CECs) is funded by the Chilean Government through the Centers of Excellence Base Financing Program of Conicyt. A.N is supported by ANID-Subdirección de Capital Humano/Doctorado Nacional/2025-21253071. M.M. thanks Silvia Trabucco and Elena Poli for very useful discussion.

IX. APPENDIX

Here we give more details on the calculation of the single noncentral vortex angular momentum reported in

Fig. 7. In analogy with Eq. (54), the number density is

$$n_I = 16K\mu_I \frac{|\mathbf{r} - \mathbf{r}_v|^{2n}}{(1 + |\mathbf{r} - \mathbf{r}_v|^{2n})^2}, \quad (96)$$

where \mathbf{r}_v is the vortex radial position from the axis of the cylinder. It is convenient to take a reference frame centered at the vortex core, O_v , so that

$$n_I = 16K\mu_I \frac{r^{2n}}{(1 + r^{2n})^2}, \quad (97)$$

while the axis of the cylinder passes through O , see Fig. 10. The angular momentum with respect to the axis of the cylinder is then given by

$$L_z = \int d^3r (\mathbf{r}' \times \mathbf{T})_z, \quad (98)$$

where $\mathbf{r}' = \mathbf{r} - \mathbf{r}_v$ and $\mathbf{T} = (0, T_{0\varphi})$, because there is no momentum flux emanating from the vortex center. We obtain that

$$L_z = L_z^1 + L_z^2, \quad (99)$$

where

$$L_z^1 = n \int d^3r r n_I, \quad (100)$$

and

$$L_z^2 = - \int d^3r (\mathbf{r}_v \times \mathbf{T})_z. \quad (101)$$

Both integrals can be evaluated as follows:

$$L_z^1 = n \int d^3r r n_I = n \ell_z \int_0^{2\pi} d\varphi \int_0^{R(\varphi)} dr r n_I, \quad (102)$$

and

$$\begin{aligned} L_z^2 &= r_1 \int d^3r T_{0\varphi} \cos \varphi \\ &= n \ell_z r_1 \int_0^{2\pi} d\varphi \cos \varphi \int_0^{R(\varphi)} dr n_I, \end{aligned} \quad (103)$$

where

$$R(\varphi) = -r_v \cos \varphi + \sqrt{R^2 - r_v^2 \sin^2 \varphi}, \quad (104)$$

is the distance of the boundary from the vortex center. From Fig. 10 we have that

$$R^2 = r_v^2 + R(\varphi)^2 + 2r_v R(\varphi) \cos \varphi, \quad (105)$$

and thus the above equation follows. The integrals can be, in part, analytically solved using the change of variable in Eq. (93).

-
- [1] E. Shuryak, Strongly coupled quark-gluon plasma in heavy ion collisions, *Rev. Mod. Phys.* **89**, 035001 (2017), [arXiv:1412.8393 \[hep-ph\]](#).
- [2] R. Pasechnik and M. Šumbera, Phenomenological Review on Quark–Gluon Plasma: Concepts vs. Observations, *Universe* **3**, 7 (2017), [arXiv:1611.01533 \[hep-ph\]](#).
- [3] W. Busza, K. Rajagopal, and W. van der Schee, Heavy Ion Collisions: The Big Picture, and the Big Questions, *Ann. Rev. Nucl. Part. Sci.* **68**, 339 (2018), [arXiv:1802.04801 \[hep-ph\]](#).
- [4] A. Bzdak, S. Esumi, V. Koch, J. Liao, M. Stephanov, and N. Xu, Mapping the Phases of Quantum Chromodynamics with Beam Energy Scan, *Phys. Rept.* **853**, 1 (2020), [arXiv:1906.00936 \[nucl-th\]](#).
- [5] K. Yagi, T. Hatsuda, and Y. Miake, *Quark-Gluon Plasma* (Cambridge University Press, 2005).
- [6] J. B. Kogut and M. A. Stephanov, *The phases of quantum chromodynamics: From confinement to extreme environments*, Vol. 21 (Cambridge University Press, 2004).
- [7] N. Brambilla *et al.*, QCD and Strongly Coupled Gauge Theories: Challenges and Perspectives, *Eur. Phys. J. C* **74**, 2981 (2014), [arXiv:1404.3723 \[hep-ph\]](#).
- [8] R. Pisarski, Three Lectures on QCD Phase Transitions, *Lect. Notes Phys.* **999**, 89 (2022).
- [9] L. McLerran and R. D. Pisarski, Phases of cold, dense quarks at large N(c), *Nucl. Phys. A* **796**, 83 (2007), [arXiv:0706.2191 \[hep-ph\]](#); Y. Hidaka, L. D. McLerran, and R. D. Pisarski, Baryons and the phase diagram for a large number of colors and flavors, *Nucl. Phys. A* **808**,

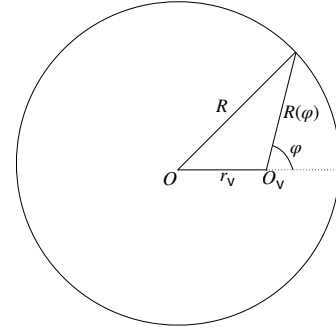


FIG. 10. Two-dimensional projection of the cylindrical system useful for the evaluation of the angular momentum of a noncentral vortex. O coincides with the axis of the cylinder while O_v indicates the vortex radial position. Both the cylinder axis and the vortex are orthogonal to the figure.

- 117 (2008), [arXiv:0803.0279 \[hep-ph\]](#).
- [10] M. G. Alford, K. Rajagopal, and F. Wilczek, QCD at finite baryon density: Nucleon droplets and color superconductivity, *Phys. Lett. B* **422**, 247 (1998), [arXiv:hep-ph/9711395 \[hep-ph\]](#).
- [11] K. Rajagopal and F. Wilczek, The condensed matter physics of qcd, in *At the Frontier of Particle Physics:*

- Handbook of QCD*, edited by M. Shifman (World Scientific, Singapore, 2001) pp. 2061–2151, [arXiv:hep-ph/0011333 \[hep-ph\]](#).
- [12] M. G. Alford, A. Schmitt, K. Rajagopal, and T. Schafer, Color superconductivity in dense quark matter, *Rev. Mod. Phys.* **80**, 1455 (2008), [arXiv:0709.4635 \[hep-ph\]](#).
- [13] R. Anglani, R. Casalbuoni, M. Ciminale, N. Ippolito, R. Gatto, *et al.*, Crystalline color superconductors, *Rev. Mod. Phys.* **86**, 509 (2014), [arXiv:1302.4264 \[hep-ph\]](#).
- [14] Y. Aoki, G. Endrodi, Z. Fodor, S. D. Katz, and K. K. Szabo, The Order of the quantum chromodynamics transition predicted by the standard model of particle physics, *Nature* **443**, 675 (2006), [arXiv:hep-lat/0611014](#).
- [15] T. Bhattacharya *et al.*, QCD Phase Transition with Chiral Quarks and Physical Quark Masses, *Phys. Rev. Lett.* **113**, 082001 (2014), [arXiv:1402.5175 \[hep-lat\]](#).
- [16] K. Nagata, Finite-density lattice QCD and sign problem: Current status and open problems, *Prog. Part. Nucl. Phys.* **127**, 103991 (2022), [arXiv:2108.12423 \[hep-lat\]](#).
- [17] N. Y. Astrakhantsev, V. V. Braguta, N. V. Kolomojets, A. Y. Kotov, D. D. Kuznedev, A. A. Nikolaev, and A. Roenko, Lattice Study of QCD Properties under Extreme Conditions: Temperature, Density, Rotation, and Magnetic Field, *Phys. Part. Nucl.* **52**, 536 (2021).
- [18] N. Astrakhantsev, V. Braguta, M. Cardinali, M. D’Elia, L. Maio, F. Sanfilippo, A. Trunin, and A. Vasiliev, Electromagnetic conductivity of quark-gluon plasma at non-zero baryon density, *PoS LATTICE2021*, 119 (2022), [arXiv:2110.10727 \[hep-lat\]](#).
- [19] B. B. Brandt, F. Cuteri, G. Endrődi, G. Markó, L. Sandbote, and A. D. M. Valois, Thermal QCD in a non-uniform magnetic background, *JHEP* **11** (229), [arXiv:2305.19029 \[hep-lat\]](#).
- [20] K. Yagi, T. Hatsuda, and Y. Miake, *Quark-gluon plasma: From big bang to little bang*, Vol. 23 (Cambridge University Press, 2005).
- [21] P. de Forcrand, Simulating QCD at finite density, *PoS LAT2009*, 010 (2009), [arXiv:1005.0539 \[hep-lat\]](#).
- [22] M. G. Alford, A. Kapustin, and F. Wilczek, Imaginary chemical potential and finite fermion density on the lattice, *Phys. Rev. D* **59**, 054502 (1999), [arXiv:hep-lat/9807039 \[hep-lat\]](#).
- [23] A. B. Migdal, Stability of vacuum and limiting fields, *Zh. Eksp. Teor. Fiz.* **61**, 2209 (1971).
- [24] A. B. Migdal, Vacuum stability and limiting fields, *Soviet Physics Uspekhi* **14**, 813 (1972).
- [25] R. F. Sawyer, Condensed pi- phase in neutron star matter, *Phys. Rev. Lett.* **29**, 382 (1972).
- [26] D. J. Scalapino, Pi- condensate in dense nuclear matter, *Phys. Rev. Lett.* **29**, 386 (1972).
- [27] J. Kogut and J. T. Manassah, π^- condensation and neutron star cooling, *Phys. Lett. A* **41**, 129 (1972).
- [28] M. Mannarelli, Meson Condensation, *Particles* **2**, 411 (2019), [arXiv:1908.02042 \[hep-ph\]](#).
- [29] G. Baym and D. K. Campbell, CHIRAL SYMMETRY AND PION CONDENSATION (1978).
- [30] D. B. Kaplan and A. E. Nelson, Strange Goings on in Dense Nucleonic Matter, *Phys. Lett. B* **175**, 57 (1986).
- [31] C. Dominguez, M. Loewe, and J. Rojas, Pion and nucleon thermal widths in the linear sigma model, *Phys. Lett.* **B320**, 377 (1994).
- [32] D. Son and M. A. Stephanov, QCD at finite isospin density, *Phys. Rev. Lett.* **86**, 592 (2001), [arXiv:hep-ph/0005225 \[hep-ph\]](#).
- [33] J. Kogut and D. Toublan, QCD at small nonzero quark chemical potentials, *Phys. Rev. D* **64**, 034007 (2001), [arXiv:hep-ph/0103271 \[hep-ph\]](#).
- [34] M. C. Birse, T. D. Cohen, and J. A. McGovern, Phases of QCD with nonvanishing isospin density, *Phys. Lett. B* **516**, 27 (2001), [arXiv:hep-ph/0104282](#).
- [35] K. Splittorff, D. Toublan, and J. J. M. Verbaarschot, Thermodynamics of chiral symmetry at low densities, *Nucl. Phys. B* **639**, 524 (2002), [arXiv:hep-ph/0204076](#).
- [36] M. Loewe and C. Villavicencio, Thermal pions at finite isospin chemical potential, *Phys. Rev. D* **67**, 074034 (2003), [arXiv:hep-ph/0212275 \[hep-ph\]](#).
- [37] M. Loewe and C. Villavicencio, Thermal pion masses in the second phase: $|\mu(I)| > m(\pi)$, *Phys. Rev. D* **70**, 074005 (2004), [arXiv:hep-ph/0404232 \[hep-ph\]](#).
- [38] M. Loewe and C. Villavicencio, Pion stability in a hot dense media, *arXiv e-Print* (2011), [arXiv:1107.3859 \[hep-ph\]](#).
- [39] A. Mammarella and M. Mannarelli, Intriguing aspects of meson condensation, *Phys. Rev. D* **92**, 085025 (2015), [arXiv:1507.02934 \[hep-ph\]](#).
- [40] S. Carignano, A. Mammarella, and M. Mannarelli, Equation of state of imbalanced cold matter from chiral perturbation theory, *Phys. Rev. D* **93**, 051503 (2016), [arXiv:1602.01317 \[hep-ph\]](#).
- [41] M. Loewe, A. Raya, and C. Villavicencio, Metastable pions in dense media, *Phys. Rev. D* **95**, 096013 (2017), [arXiv:1610.05751 \[hep-ph\]](#).
- [42] S. Carignano, L. Lepori, A. Mammarella, M. Mannarelli, and G. Pagliaroli, Scrutinizing the pion condensed phase, *Eur. Phys. J. A* **53**, 35 (2017), [arXiv:1610.06097 \[hep-ph\]](#).
- [43] L. Lepori and M. Mannarelli, Multicomponent meson superfluids in chiral perturbation theory, *Phys. Rev. D* **99**, 096011 (2019), [arXiv:1901.07488 \[hep-ph\]](#).
- [44] P. Adhikari, J. O. Andersen, and P. Kneschke, Two-flavor chiral perturbation theory at nonzero isospin: Pion condensation at zero temperature, *Eur. Phys. J. C* **79**, 874 (2019), [arXiv:1904.03887 \[hep-ph\]](#).
- [45] A. N. Tawfik, A. M. Diab, M. T. Ghoneim, and H. Anwer, SU(3) Polyakov Linear-Sigma Model With Finite Isospin Asymmetry: QCD Phase Diagram, *Int. J. Mod. Phys. A* **34**, 1950199 (2019), [arXiv:1904.09890 \[hep-ph\]](#).
- [46] I. N. Mishustin, D. V. Anchishkin, L. M. Satarov, O. S. Stashko, and H. Stoecker, Condensation of interacting scalar bosons at finite temperatures, *Phys. Rev. C* **100**, 022201 (2019), [arXiv:1905.09567 \[nucl-th\]](#).
- [47] A. Barducci, R. Casalbuoni, S. De Curtis, R. Gatto, and G. Pettini, Pion Decay Constant at Finite Temperature and Density, *Phys. Rev. D* **42**, 1757 (1990).
- [48] D. Toublan and J. Kogut, Isospin chemical potential and the QCD phase diagram at nonzero temperature and baryon chemical potential, *Phys. Lett. B* **564**, 212 (2003), [arXiv:hep-ph/0301183 \[hep-ph\]](#).
- [49] A. Barducci, R. Casalbuoni, G. Pettini, and L. Ravagli, A Calculation of the QCD phase diagram at finite temperature, and baryon and isospin chemical potentials, *Phys. Rev. D* **69**, 096004 (2004), [arXiv:hep-ph/0402104 \[hep-ph\]](#).
- [50] A. Barducci, R. Casalbuoni, G. Pettini, and L. Ravagli, Pion and kaon condensation in a 3-flavor NJL model, *Phys. Rev. D* **71**, 016011 (2005), [arXiv:hep-ph/0410250 \[hep-ph\]](#).

- [51] L.-Y. He, M. Jin, and P.-F. Zhuang, Pion superfluidity and meson properties at finite isospin density, *Phys. Rev. D* **71**, 116001 (2005), [arXiv:hep-ph/0503272 \[hep-ph\]](#).
- [52] D. Ebert and K. G. Klimenko, Gapless pion condensation in quark matter with finite baryon density, *J. Phys. G* **32**, 599 (2006), [arXiv:hep-ph/0507007 \[hep-ph\]](#).
- [53] D. Ebert and K. G. Klimenko, Pion condensation in electrically neutral cold matter with finite baryon density, *Eur. Phys. J. C* **46**, 771 (2006), [arXiv:hep-ph/0510222 \[hep-ph\]](#).
- [54] S. Mukherjee, M. G. Mustafa, and R. Ray, Thermodynamics of the PNJL model with nonzero baryon and isospin chemical potentials, *Phys. Rev. D* **75**, 094015 (2007), [arXiv:hep-ph/0609249](#).
- [55] L. He and P. Zhuang, Phase structure of Nambu-Jona-Lasinio model at finite isospin density, *Phys. Lett. B* **615**, 93 (2005), [arXiv:hep-ph/0501024](#).
- [56] L. He, M. Jin, and P. Zhuang, Pion Condensation in Baryonic Matter: from Sarma Phase to Larkin-Ovchinnikov-Fudde-Ferrell Phase, *Phys. Rev. D* **74**, 036005 (2006), [arXiv:hep-ph/0604224](#).
- [57] G.-f. Sun, L. He, and P. Zhuang, BEC-BCS crossover in the Nambu-Jona-Lasinio model of QCD, *Phys. Rev. D* **75**, 096004 (2007), [arXiv:hep-ph/0703159](#).
- [58] J. O. Andersen and L. Kyllingstad, Pion Condensation in a two-flavor NJL model: the role of charge neutrality, *J. Phys. G* **37**, 015003 (2009), [arXiv:hep-ph/0701033](#).
- [59] H. Abuki, M. Ciminale, R. Gatto, N. D. Ippolito, G. Nardulli, and M. Ruggieri, Electrical neutrality and pion modes in the two flavor PNJL model, *Phys. Rev. D* **78**, 014002 (2008), [arXiv:0801.4254 \[hep-ph\]](#).
- [60] H. Abuki, R. Anglani, R. Gatto, M. Pellicoro, and M. Ruggieri, The Fate of pion condensation in quark matter: From the chiral to the real world, *Phys. Rev. D* **79**, 034032 (2009), [arXiv:0809.2658 \[hep-ph\]](#).
- [61] C.-f. Mu, L.-y. He, and Y.-x. Liu, Evaluating the phase diagram at finite isospin and baryon chemical potentials in the Nambu-Jona-Lasinio model, *Phys. Rev. D* **82**, 056006 (2010).
- [62] T. Xia, L. He, and P. Zhuang, Three-flavor Nambu-Jona-Lasinio model at finite isospin chemical potential, *Phys. Rev. D* **88**, 056013 (2013), [arXiv:1307.4622 \[hep-ph\]](#).
- [63] T. Xia and P. Zhuang, Quark-antiquark scattering phase shift and meson spectral function in pion superfluid, *Chinese Physics C* (2014), [arXiv:1411.6713 \[hep-ph\]](#).
- [64] J. Chao, M. Huang, and A. Radzhabov, Charged pion condensation in anti-parallel electromagnetic fields and nonzero isospin density, *Chin. Phys. C* **44**, 034105 (2020), [arXiv:1805.00614 \[hep-ph\]](#).
- [65] T. G. Khunjua, K. G. Klimenko, and R. N. Zhokhov, Chiral imbalanced hot and dense quark matter: NJL analysis at the physical point and comparison with lattice QCD, *Eur. Phys. J. C* **79**, 151 (2019), [arXiv:1812.00772 \[hep-ph\]](#).
- [66] T. G. Khunjua, K. G. Klimenko, and R. N. Zhokhov, Dualities and inhomogeneous phases in dense quark matter with chiral and isospin imbalances in the framework of effective model, *JHEP* **06**, 006, [arXiv:1901.02855 \[hep-ph\]](#).
- [67] T. Khunjua, K. Klimenko, and R. Zhokhov, Charged Pion Condensation in Dense Quark Matter: Nambu-Jona-Lasinio Model Study, *Symmetry* **11**, 778 (2019), [arXiv:1912.08635 \[hep-ph\]](#).
- [68] S. S. Avancini, A. Bandyopadhyay, D. C. Duarte, and R. L. S. Farias, Cold QCD at finite isospin density: confronting effective models with recent lattice data, *Phys. Rev. D* **100**, 116002 (2019), [arXiv:1907.09880 \[hep-ph\]](#).
- [69] Z.-Y. Lu, C.-J. Xia, and M. Ruggieri, Thermodynamics and susceptibilities of isospin imbalanced QCD matter, *Eur. Phys. J. C* **80**, 46 (2020), [arXiv:1907.11497 \[hep-ph\]](#).
- [70] J. P. Carlomagno, D. Gomez Dumm, and N. N. Scoccola, Cold isospin asymmetric baryonic rich matter in nonlocal NJL-like models, *Phys. Rev. D* **109**, 094041 (2024), [arXiv:2402.13842 \[hep-ph\]](#).
- [71] S. P. Klevansky, The Nambu-Jona-Lasinio model of quantum chromodynamics, *Rev. Mod. Phys.* **64**, 649 (1992).
- [72] J. O. Andersen, W. R. Naylor, and A. Tranberg, Phase diagram of QCD in a magnetic field: A review, *Rev. Mod. Phys.* **88**, 025001 (2016), [arXiv:1411.7176 \[hep-ph\]](#).
- [73] P. Adhikari, J. O. Andersen, and P. Kneschke, On-shell parameter fixing in the quark-meson model, *Phys. Rev. D* **95**, 036017 (2017), [arXiv:1612.03668 \[hep-ph\]](#).
- [74] P. Adhikari, J. O. Andersen, and P. Kneschke, Pion condensation and phase diagram in the Polyakov-loop quark-meson model, *Phys. Rev. D* **98**, 074016 (2018), [arXiv:1805.08599 \[hep-ph\]](#).
- [75] J. O. Andersen and P. Kneschke, Chiral density wave versus pion condensation at finite density and zero temperature, *Phys. Rev. D* **97**, 076005 (2018), [arXiv:1802.01832 \[hep-ph\]](#).
- [76] J. O. Andersen, P. Adhikari, and P. Kneschke, Pion condensation and QCD phase diagram at finite isospin density, *PoS Confinement2018*, 197 (2019), [arXiv:1810.00419 \[hep-ph\]](#).
- [77] B. B. Brandt, V. Chelnokov, G. Endrodi, G. Marko, D. Scheid, and L. von Smekal, Renormalization group invariant mean-field model for QCD at finite isospin density, *Phys. Rev. D* **112**, 054038 (2025), [arXiv:2502.04025 \[hep-ph\]](#).
- [78] B. Klein, D. Toublan, and J. J. M. Verbaarschot, The QCD phase diagram at nonzero temperature, baryon and isospin chemical potentials in random matrix theory, *Phys. Rev. D* **68**, 014009 (2003), [arXiv:hep-ph/0301143](#).
- [79] B. Klein, D. Toublan, and J. Verbaarschot, Diquark and pion condensation in random matrix models for two color QCD, *Phys.Rev. D* **72**, 015007 (2005), [arXiv:hep-ph/0405180 \[hep-ph\]](#).
- [80] A. Barducci, G. Pettini, L. Ravagli, and R. Casalbuoni, Ladder QCD at finite isospin chemical potential, *Phys. Lett. B* **564**, 217 (2003), [arXiv:hep-ph/0304019](#).
- [81] M. Lv, D. Li, and S. He, Pion condensation in a soft-wall AdS/QCD model, *JHEP* **11**, 026, [arXiv:1811.03828 \[hep-ph\]](#).
- [82] N. Kovensky and A. Schmitt, Isospin asymmetry in holographic baryonic matter, *SciPost Phys.* **11**, 029 (2021), [arXiv:2105.03218 \[hep-ph\]](#).
- [83] Y. Chen, M. Ding, D. Li, K. Bitaghsir Fadafan, and M. Huang, Pion condensation and pion star from holographic QCD, *Phys. Rev. D* **111**, 126010 (2025), [arXiv:2408.17080 \[hep-ph\]](#).

- [84] J. B. Kogut and D. K. Sinclair, Quenched lattice QCD at finite isospin density and related theories, *Phys. Rev. D* **66**, 014508 (2002), [arXiv:hep-lat/0201017](#).
- [85] J. B. Kogut and D. K. Sinclair, Lattice QCD at finite isospin density at zero and finite temperature, *Phys. Rev. D* **66**, 034505 (2002), [arXiv:hep-lat/0202028 \[hep-lat\]](#).
- [86] J. B. Kogut and D. K. Sinclair, The Finite temperature transition for 2-flavor lattice QCD at finite isospin density, *Phys. Rev. D* **70**, 094501 (2004), [arXiv:hep-lat/0407027](#).
- [87] S. R. Beane, W. Detmold, T. C. Luu, K. Orginos, M. J. Savage, and A. Torok, Multi-Pion Systems in Lattice QCD and the Three-Pion Interaction, *Phys. Rev. Lett.* **100**, 082004 (2008), [arXiv:0710.1827 \[hep-lat\]](#).
- [88] P. de Forcrand, M. A. Stephanov, and U. Wenger, On the phase diagram of QCD at finite isospin density, *PoS LATTICE2007*, 237 (2007), [arXiv:0711.0023 \[hep-lat\]](#).
- [89] W. Detmold, M. J. Savage, A. Torok, S. R. Beane, T. C. Luu, K. Orginos, and A. Parreno, Multi-Pion States in Lattice QCD and the Charged-Pion Condensate, *Phys. Rev. D* **78**, 014507 (2008), [arXiv:0803.2728 \[hep-lat\]](#).
- [90] W. Detmold, K. Orginos, M. J. Savage, and A. Walker-Loud, Kaon Condensation with Lattice QCD, *Phys. Rev. D* **78**, 054514 (2008), [arXiv:0807.1856 \[hep-lat\]](#).
- [91] W. Detmold and B. Smigielski, Lattice QCD study of mixed systems of pions and kaons, *Phys. Rev. D* **84**, 014508 (2011), [arXiv:1103.4362 \[hep-lat\]](#).
- [92] W. Detmold, K. Orginos, and Z. Shi, Lattice QCD at non-zero isospin chemical potential, *Phys. Rev. D* **86**, 054507 (2012), [arXiv:1205.4224 \[hep-lat\]](#).
- [93] P. Cea, L. Cosmai, M. D'Elia, A. Papa, and F. Sanfilippo, The critical line of two-flavor QCD at finite isospin or baryon densities from imaginary chemical potentials, *Phys. Rev. D* **85**, 094512 (2012), [arXiv:1202.5700 \[hep-lat\]](#).
- [94] G. Endrödi, Magnetic structure of isospin-asymmetric QCD matter in neutron stars, *Phys. Rev. D* **90**, 094501 (2014), [arXiv:1407.1216 \[hep-lat\]](#).
- [95] O. Janssen, M. Kieburg, K. Splittorff, J. J. M. Verbaarschot, and S. Zafeiropoulos, Phase Diagram of Dynamical Twisted Mass Wilson Fermions at Finite Isospin Chemical Potential, *Phys. Rev. D* **93**, 094502 (2016), [arXiv:1509.02760 \[hep-lat\]](#).
- [96] B. B. Brandt and G. Endrodi, QCD phase diagram with isospin chemical potential, *PoS LATTICE2016*, 039 (2016), [arXiv:1611.06758 \[hep-lat\]](#).
- [97] B. B. Brandt and G. Endrodi, Reliability of Taylor expansions in QCD, *Phys. Rev. D* **99**, 014518 (2019), [arXiv:1810.11045 \[hep-lat\]](#).
- [98] B. B. Brandt, G. Endrodi, and S. Schmalzbauer, QCD at finite isospin chemical potential, *EPJ Web Conf.* **175**, 07020 (2018), [arXiv:1709.10487 \[hep-lat\]](#).
- [99] B. B. Brandt, G. Endrodi, and S. Schmalzbauer, QCD at nonzero isospin asymmetry (2018) [arXiv:1811.06004 \[hep-lat\]](#).
- [100] B. B. Brandt, F. Cuteri, and G. Endrodi, Equation of state and speed of sound of isospin-asymmetric QCD on the lattice, *JHEP* **07**, 055, [arXiv:2212.14016 \[hep-lat\]](#).
- [101] B. B. Brandt, V. Chelnokov, F. Cuteri, and G. Endrödi, QCD phase structure at finite isospin chemical potential and smaller-than-physical quark mass, in *31st International Conference on Ultra-relativistic Nucleus-Nucleus Collisions* (2025) [arXiv:2512.05789 \[hep-lat\]](#).
- [102] T. Graf, J. Schaffner-Bielich, and E. S. Fraga, Perturbative thermodynamics at nonzero isospin density for cold QCD, *Phys. Rev. D* **93**, 085030 (2016), [arXiv:1511.09457 \[hep-ph\]](#).
- [103] J. O. Andersen, N. Haque, M. G. Mustafa, and M. Strickland, Three-loop hard-thermal-loop perturbation theory thermodynamics at finite temperature and finite baryonic and isospin chemical potential, *Phys. Rev. D* **93**, 054045 (2016), [arXiv:1511.04660 \[hep-ph\]](#).
- [104] I. Danhoni, Y. Yang, M. Hippert, and J. Noronha-Hostler, Symmetry energy of 2+1-flavor dense quark matter from perturbative qcd (2025), preprint, [arXiv:2510.23984 \[nucl-th\]](#).
- [105] N. S. Manton and P. Sutcliffe, *Topological solitons*, Cambridge Monographs on Mathematical Physics (Cambridge University Press, 2004).
- [106] M. Shifman, *Advanced topics in quantum field theory.: A lecture course* (Cambridge Univ. Press, Cambridge, UK, 2012).
- [107] E. Shuryak, *Nonperturbative Topological Phenomena in QCD and Related Theories*, Lecture Notes in Physics, Vol. 977 (Springer Nature, 2021).
- [108] E. J. Weinberg, *Classical solutions in quantum field theory: Solitons and Instantons in High Energy Physics*, Cambridge Monographs on Mathematical Physics (Cambridge University Press, 2012).
- [109] N. S. Manton, A Remark on the Scattering of BPS Monopoles, *Phys. Lett. B* **110**, 54 (1982); Monopole Interactions at Long Range, *Phys. Lett. B* **154**, 397 (1985), [Erratum: *Phys.Lett.B* 157, 475 (1985)].
- [110] N. S. Manton and S. M. Nasir, Volume of vortex moduli spaces, *Commun. Math. Phys.* **199**, 591 (1999), [arXiv:hep-th/9807017](#).
- [111] G. W. Gibbons and N. S. Manton, The Moduli space metric for well separated BPS monopoles, *Phys. Lett. B* **356**, 32 (1995), [arXiv:hep-th/9506052](#).
- [112] E. P. Gross, Structure of a quantized vortex in boson systems, *Il Nuovo Cimento* (1955-1965) **20**, 454 (1961).
- [113] L. Pitaevskii, Vortex lines in an imperfect Bose gas, *Sov. Phys. JETP* **13**, 451 (1961).
- [114] F. Dalfovo, S. Giorgini, L. P. Pitaevskii, and S. Stringari, Theory of Bose-Einstein condensation in trapped gases, *Rev. Mod. Phys.* **71**, 463 (1999).
- [115] A. Schmitt, *Introduction to Superfluidity: Field-theoretical approach and applications*, Vol. 888 (Springer International Publishing, 2015) [arXiv:1404.1284 \[hep-ph\]](#).
- [116] S. Stringari and L. Pitaevskii, *Bose-Einstein condensation and superfluidity* (Oxford Science Publications, Oxford, 2016).
- [117] F. Canfora and P. Pais, Fractional vorticity, Bogomol'nyi-Prasad-Sommerfield systems and complex structures for the (generalized) spinor Gross-Pitaevskii equations, *Nucl. Phys. B* **1017**, 116955 (2025), [arXiv:2502.00578 \[cond-mat.quant-gas\]](#).
- [118] F. Canfora and P. Pais, A Bogomol'nyi-Prasad-Sommerfield bound with a first-order system in the 2D Gross-Pitaevskii equation, *Eur. Phys. J. C* **85**, 884 (2025), [arXiv:2501.04092 \[cond-mat.quant-gas\]](#).
- [119] A. Comtet and G. Gibbons, Bogomol'nyi bounds for cosmic strings, *Nuclear Physics B* **299**, 719 (1988).
- [120] F. Canfora, A. Gomberoff, C. Henríquez-Baez, and A. Vera, Exact black holes and black branes with

- bumpy horizons supported by superfluid pions, (2026), [arXiv:2601.22914 \[hep-th\]](#).
- [121] F. Canfora, Magnetized Baryonic layer and a novel BPS bound in the gauged-non-linear-sigma-model-Maxwell theory in (3+1)-dimensions through Hamilton-Jacobi equation, *JHEP* **11** (007), [arXiv:2309.03153 \[hep-th\]](#).
- [122] F. Canfora, M. Lagos, and A. Vera, Superconducting multi-vortices and a novel BPS bound in chiral perturbation theory, *JHEP* **10** (224), [arXiv:2405.08082 \[hep-th\]](#).
- [123] S. Weinberg, Phenomenological lagrangians, *Physica A: Statistical Mechanics and its Applications* **96**, 327 (1979).
- [124] J. Gasser and H. Leutwyler, Chiral Perturbation Theory to One Loop, *Ann. Phys.* **158**, 142 (1984).
- [125] H. Georgi, *Weak Interactions and Modern Particle Theory*, Dover Books on Physics Series (Dover Publications, 2009).
- [126] H. Leutwyler, On the foundations of chiral perturbation theory, *Ann. Phys.* **235**, 165 (1994), [arXiv:hep-ph/9311274 \[hep-ph\]](#).
- [127] G. Ecker, Chiral perturbation theory, *Prog. Part. Nucl. Phys.* **35**, 1 (1995), [arXiv:hep-ph/9501357 \[hep-ph\]](#).
- [128] H. Leutwyler, Phonons as goldstone bosons, *Helv. Phys. Acta* **70**, 275 (1997), [arXiv:hep-ph/9609466 \[hep-ph\]](#).
- [129] A. Pich, Effective field theory: Course, in *Probing the standard model of particle interactions. Proceedings, Summer School in Theoretical Physics, NATO Advanced Study Institute, 68th session, Les Houches, France, July 28-September 5, 1997. Pt. 1, 2* (1998) pp. 949–1049, [arXiv:hep-ph/9806303 \[hep-ph\]](#).
- [130] S. Scherer, Introduction to chiral perturbation theory, *Adv. Nucl. Phys.* **27**, 277 (2003), [arXiv:hep-ph/0210398 \[hep-ph\]](#).
- [131] S. Scherer and M. R. Schindler, A chiral perturbation theory primer, *Prog. Part. Nucl. Phys.* **64**, 1 (2010), [arXiv:hep-ph/0505265 \[hep-ph\]](#).
- [132] T. Kojo and D. Suenaga, Peaks of sound velocity in two color dense QCD: Quark saturation effects and semishort range correlations, *Phys. Rev. D* **105**, 076001 (2022), [arXiv:2110.02100 \[hep-ph\]](#).
- [133] L. Pitaevskii and S. Stringari, *Bose-Einstein Condensation and Superfluidity* (Oxford University Press, Oxford, 2016).
- [134] E. B. Bogomolny, Stability of Classical Solutions, *Sov. J. Nucl. Phys.* **24**, 449 (1976).
- [135] A. Yamamoto and Y. Hirono, Lattice QCD in rotating frames, *Phys. Rev. Lett.* **111**, 081601 (2013), [arXiv:1303.6292 \[hep-lat\]](#).
- [136] X.-G. Huang, K. Nishimura, and N. Yamamoto, Anomalous effects of dense matter under rotation, *JHEP* **02**, 069, [arXiv:1711.02190 \[hep-ph\]](#).
- [137] H. Zhang, D. Hou, and J. Liao, Mesonic Condensation in Isospin Matter under Rotation, *Chin. Phys. C* **44**, 111001 (2020), [arXiv:1812.11787 \[hep-ph\]](#).
- [138] G. W. Evans, N. Yamamoto, and D.-L. Yang, Vorticity-induced effects from Wess-Zumino-Witten terms, (2025), [arXiv:2510.25459 \[hep-ph\]](#).
- [139] B. B. Brandt, G. Endrődi, E. S. Fraga, M. Hippert, J. Schaffner-Bielich, and S. Schmalzbauer, New class of compact stars: Pion stars, *Phys. Rev. D* **98**, 094510 (2018).
- [140] J. O. Andersen and P. Kneschke, Bose-Einstein condensation and pion stars, [arXiv:1807.08951 \[hep-ph\]](#).
- [141] O. S. Stashko, O. V. Savchuk, L. M. Satarov, I. N. Mishustin, M. I. Gorenstein, and V. I. Zhdanov, Pion stars embedded in neutrino clouds, *Phys. Rev. D* **107**, 114025 (2023), [arXiv:2303.06190 \[hep-ph\]](#).
- [142] R. Kirichenkov, J. Kunz, N. Sawado, and Y. Shnir, Skyrmions and pion stars in the gauged U(1) Einstein-Skyrme model, *Phys. Rev. D* **109**, 045002 (2024), [arXiv:2311.12432 \[hep-th\]](#).
- [143] L. Cipriani, M. Mannarelli, F. Nesti, and S. Trabucchi, Superfluid dark stars, *Phys. Rev. D* **110**, L021301 (2024), [arXiv:2403.03833 \[astro-ph.CO\]](#).
- [144] S. Shapiro and S. Teukolsky, *Black holes, white dwarfs, and neutron stars: the physics of compact objects*, A Wiley-interscience publication (Wiley, New York, USA, 1983).